PART III

Subsystems

CHAPTER

9

Radar Antennas

Christopher D. Bailey

Chapter Outline

9.1 INTRODUCTION

The radar antenna is responsible for transmitting electromagnetic energy into the environment and receiving energy that has reflected off a distant target. To perform this job efficiently, the radar antenna must (1) provide a matched interface between the transmitter (TX), receiver (RX), and free space, and (2) provide angular selectivity for energy being transmitted and received from the radar. These functions are illustrated in Figure 9-1.

In this chapter the primary features of the antenna will be presented, and their effect on performance will be discussed. Operational and performance issues associated with the two

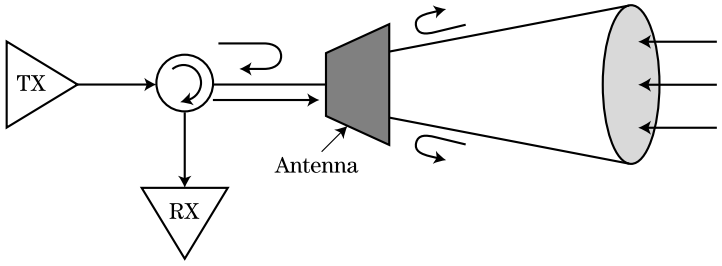

FIGURE 9-1 ■ The radar antenna must provide angular selectivity and a good electrical match.

most important classes of radar antennas, the reflector and phased array, will be described. Emphasis will not be on antenna design, which is widely covered in the literature [1–3], but on salient antenna features and characteristics that every radar engineer should understand.

9.2 BASIC ANTENNA CONCEPTS

9.2.1 The Isotropic Antenna

This introduction to the radar antenna will begin with the isotropic antenna, which is a theoretical point source that transmits and receives energy equally in all directions (Figure 9-2). This fictional antenna is an important reference for describing the radiation properties of all other antennas and will serve as a departure point.

As shown in Figure 9-2, the isotropic antenna radiates equally in all directions and therefore has no angular selectivity. The radiation intensity (watts/steradian) from an isotropic antenna can be written as

$$I = \frac{P_t}{4\pi} \tag{9.1}$$

where P_t is the total power radiated by the antenna and 4π is the steradian area of the sphere enclosing the antenna. The power density (W/m^2) measured at a distance R from the isotropic antenna is

$$Q_t = \frac{P_t}{4\pi R^2} \tag{9.2}$$

Since the area of the sphere surrounding the antenna grows as R^2, the power density must decrease as $1/R^2$. The circular lines in Figure 9-2 represent locations of equal radiated intensity and phase. The solid and dashed lines represent propagating wave fronts spaced

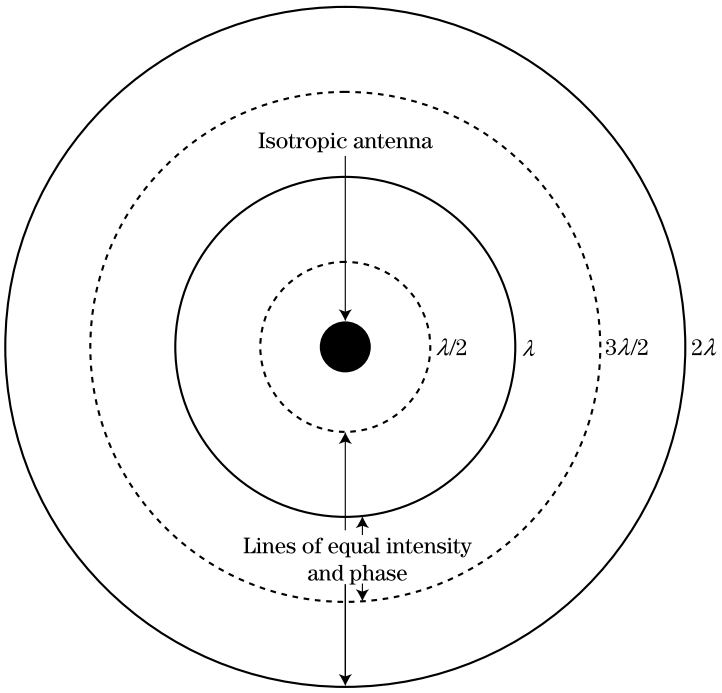

FIGURE 9-2 ■ The isotropic antenna radiates equally in all directions. The concentric rings indicate spheres of equal phase and radiation intensity.

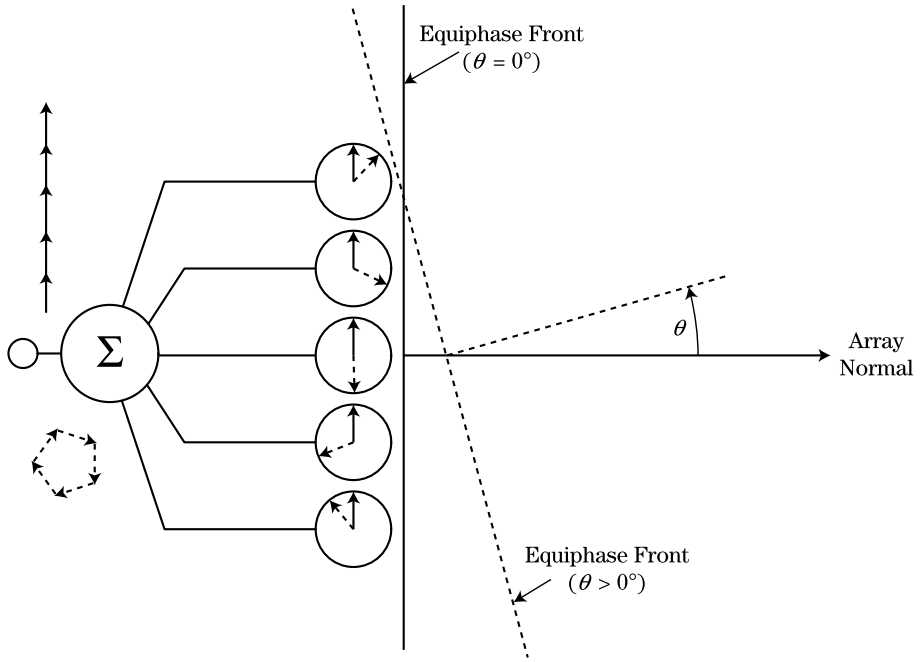

FIGURE 9-3 ■ The response of an array to an incoming plane wave is the sum of the element excitation vectors, which will combine constructively or destructively depending upon the incidence angle.

at one-half wavelength intervals. The phase of the electromagnetic wave at adjacent lines will therefore differ by 180° at any given time.

9.2.2 The Radiation Pattern

In contrast to an ideal isotropic antenna, the radiated energy from a radar antenna is highly dependent on angle. In fact, one purpose of an antenna is to concentrate the radiated energy into a narrow angular region. There are different types of radar antennas, and considerable discussion will be given to these later in the chapter. For now, a simple array of isotropic antennas will be used to explain this angular dependence. Figure 9-3 shows an array of five isotropic antennas (elements) connected at a common node referred to as the summation point. The summation point is the location where the individual element signals combine and the total antenna response is measured. This figure also depicts two plane waves incident on the radiating surface from different angles θ with respect to the normal to the array surface, or "array normal" for short. The defining property of a plane wave is that the electric field is in phase everywhere on the plane perpendicular to the direction of propagation. Thus every location on the antenna's radiating surface will detect the same phase when $\theta = 0^\circ$. This is indicated by the solid vectors in the circles at each element location. The signal received at each antenna element will combine in phase at the summation point (assuming that the path length from each antenna element to the summation point is equal).

Now let θ be slightly greater than 0° (dashed line). This phase front reaches each element at a different moment in time, and at any instant the five elements will be experiencing different phases from the incoming plane wave. This is illustrated by the dashed excitation vectors at each antenna location. Since each element detects a different phase from the incoming plane wave, the combined energy will no longer add coherently and the amplitude of the resulting signal will be smaller than when $\theta = 0^\circ$. As θ continues to increase there will exist an angle, or multiple angles, at which the vector sum of the phase excitations will completely cancel.

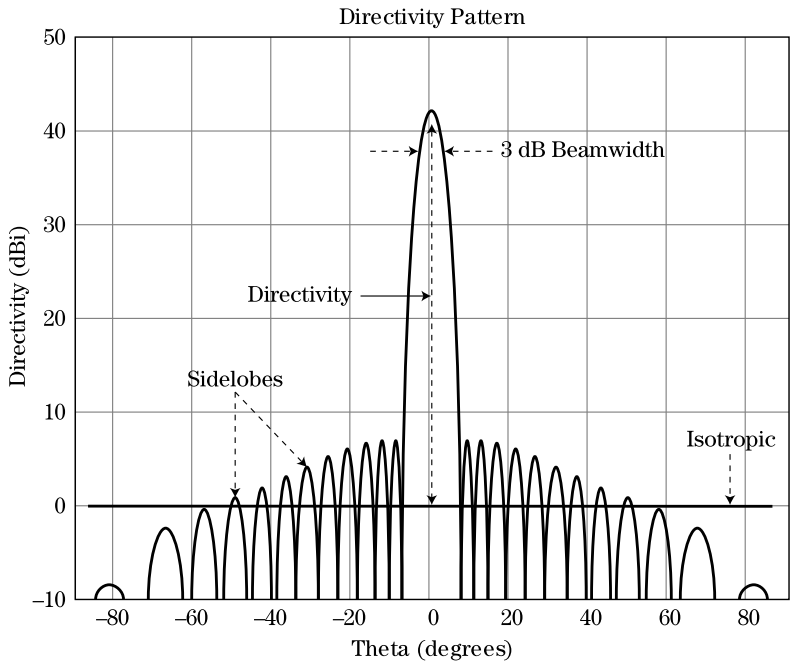

FIGURE 9-4 ■ The directivity pattern of a radar antenna and some related parameters.

Figure 9-4 shows the signal strength as a function of incidence angle. This figure shows a typical radiation pattern structure for an antenna in which energy is collected over a large surface area. The maximum of this plot, or main beam peak, occurs at the angle where all collected energy coherently adds together. For the remaining angles the collected energy will either cancel to cause nulls or partially combine to create *sidelobes*.

9.2.3 Beamwidth

The pattern in Figure 9-4 is called the *radiation* or *directivity pattern* of an antenna. The angular distance from the half power (−3 dB) point on one side of the main beam to the half power point on the other side is called the 3 dB beamwidth, or simply the beamwidth. To explain this concept further requires consideration of the phase variation across the antenna from an off-axis plane wave. The phase variation across the array surface, or *aperture*, is the total path length variation times $2\pi/\lambda$. This can be written as

$$\Delta\phi = \frac{2\pi L \sin\theta}{\lambda} \tag{9.3}$$

where the length of the antenna is D. For an array of elements, D can be replaced by $n\Delta x$, where n is the total number of elements and Δx is the distance between elements.

The total phase variation across the array increases with antenna size. Thus, as size increases the antenna response changes more rapidly with respect to θ. Consequently, the main beam becomes narrower and more directional. The beamwidth of an antenna is inversely proportional to its size. In general, the beamwidth in radians is

$$\theta_3 = \frac{\alpha\lambda}{L} \tag{9.4}$$

where α is the beamwidth factor and is determined by the aperture taper function (see section 9.3) and the aperture shape. If the aperture is circular and uniformly weighted, α is approximately equal to 1.

9.2.4 Directivity and Gain

The directivity pattern describes the intensity of the energy radiated by the antenna in all angular directions (i.e., it is a function of θ). Directivity is a unitless quantity expressed as a ratio of the radiation intensity of an antenna in a particular direction to that of a lossless isotropic antenna with the same radiated power. The vertical axis in Figure 9-4 has units of dBi, or dB relative to an isotropic antenna. The maximum directivity for a planar radar antenna is [3]

$$D_{\max} = \frac{\eta_a 4\pi A}{\lambda^2} \tag{9.5}$$

where the antenna's physical aperture area is A and the aperture efficiency is η_a. As with the coefficient α, η_a is determined by the aperture taper, which is discussed in the next section. The effective aperture A_e is the product of the physical antenna size and the aperture efficiency, or $A_e = \eta_a A$. The effective aperture is a measure of how efficiently the antenna's physical area is being used. The aperture is most efficient ($\eta_a = 1$) when uniformly illuminated.

Equations 9.4 and 9.5 can be combined to describe directivity with respect to the 3 dB beamwidth. The directivity of a uniformly illuminated rectangular antenna is

$$D_{\max} \approx \frac{4\pi(0.88)^2}{\theta_3 \phi_3} \tag{9.6}$$

where θ_3 and ϕ_3 are the azimuth and elevation 3 dB beamwidths in radians. For a uniformly illuminated rectangular array $\alpha = 0.88$ and $\eta_a = 1$. Equation (9.6) shows that the maximum directivity is proportional to the ratio of the steradian area of an isotropic antenna, which radiates equally over the full 4π steradians to the steradian area of the antenna main beam.

The terms *gain* and directivity are often incorrectly used interchangeably. These terms are closely related; however, there is an important distinction. The gain of an antenna is a measure of the ratio of the radiation intensity at the peak of the main beam to that of a lossless isotropic antenna with the same input power. Therefore, gain G is equal to the maximum directivity $D_{\max}$ minus the losses internal to the antenna. Gain can never exceed the maximum directivity.

Antenna gain should not be confused with the gain of an amplifier. An amplifier with 30 dB of gain would have 1,000 times more radiofrequency (RF) power at the output than at the input. This power increase is achieved by converting direct current (DC) power to additional RF power. An antenna with 30 dB of gain will radiate 1,000 times as much power in the direction of the main beam than will an isotropic antenna with the same input power but will deliver much less power than the isotropic antenna in most other directions. The antenna gain is achieved by concentrating the power in a preferred direction, not by creating additional power.

9.2.5 Sidelobes

The radar engineer will often want to minimize energy in the sidelobe region. Strong sidelobes will increase the clutter return, increase the number of false alarms, and make the radar more susceptible to jamming. For this reason numerous metrics are used to describe the sidelobe structure of an antenna.

The peak sidelobes are usually near the main beam and are expressed in dBi or dB relative to the peak of the main beam. The unit "dBi" means decibels relative to an isotropic

antenna. In Figure 9-4, the maximum directivity is 43 dBi, and the near-in sidelobes on either side of the main beam are approximately 36 dB below the main beam peak, or 7 dBi. It is typical for a highly directive radar antenna to have peak sidelobes above the isotopic level (0 dBi). The peak sidelobe level is set by the aperture shape and the electric field distribution across the aperture.

The average sidelobe level is an important figure of merit for most radar antennas. Since the radar beam is constantly being scanned to different angular locations, the relative gain of clutter, jamming, or any other signal entering through the sidelobe region is usually assessed as a function of the average sidelobe level instead of a specific sidelobe. The average ratio of the sidelobe power to that of an isotropic antenna with the same input power is

$$SL_{ave} = \frac{\frac{P_{SL}}{\Omega_{SL}}}{\frac{P_t}{4\pi}} = \frac{(P_t - P_{MB})}{(4\pi - \Omega_{MB})} \cdot \frac{4\pi}{P_T} = \frac{\left(1 - \frac{P_{MB}}{P_t}\right)}{\left(1 - \frac{\Omega_{MB}}{4\pi}\right)} \approx 1 - \frac{P_{MB}}{P_t} \tag{9.7}$$

where P_t is the total radiated power, P_{SL} is the power radiated into the sidelobe region, P_{MB} is the power in main beam, Ω_{SL} is the steradian area of sidelobe region, and Ω_{MB} is the steradian area of main beam.

For highly directive radar antennas with a main beam of only a few degrees, Ω_{MB} is much less than 4π. Equation (9.7) then becomes a simple energy conservation equation that states the average isotropic sidelobe power is 1 minus the fraction of power in the main beam. It will be seen later that the average sidelobe level is partially determined by tolerance errors in the amplitude and phase of the electric field in the antenna's aperture. As will be discussed, aperture tapers can be used to reduce the sidelobe level; however, the minimum achievable sidelobe level is ultimately determined by errors. These errors will scatter power out of the main beam and into the sidelobe region, thereby reducing the gain and raising the average sidelobe level as indicated in equation (9.7). It can also be seen in equation (9.7) that the average sidelobe level must be below isotropic or 0 dBi.

9.3 APERTURE TAPERS

The radiating surface of an antenna is often referred to as the aperture. An antenna's aperture is defined as an opening in a plane directly in front of the antenna through which practically all the power radiated or received by the antenna passes. Figure 9-5 shows the aperture for a reflector and array antenna. The sidelobe structure of an antenna's radiation pattern can be controlled by adjusting the spatial distribution of the electric field across this aperture. This electric field distribution is called the aperture *taper*.

If the aperture taper is uniform (i.e., electric field strength is the same everywhere throughout the aperture), the antenna will have the greatest directivity and narrowest beamwidth possible; however, the peak sidelobes will be high (≈13 dB below the main beam for a rectangular aperture). The peak sidelobe can be significantly reduced by using a taper that maximizes the field strength at the center of the aperture and decreases the field strength outwardly toward the aperture edges. However, with a low sidelobe aperture taper the maximum directivity is reduced and the beamwidth is increased. A fundamental trade-off exists between maximizing directivity and decreasing sidelobe levels.[1]

[1]This same trade-off between peak directivity or gain, resolution, and sidelobe level also exists in range and Doppler sidelobe control; see Chapters 14, 17, and 20.

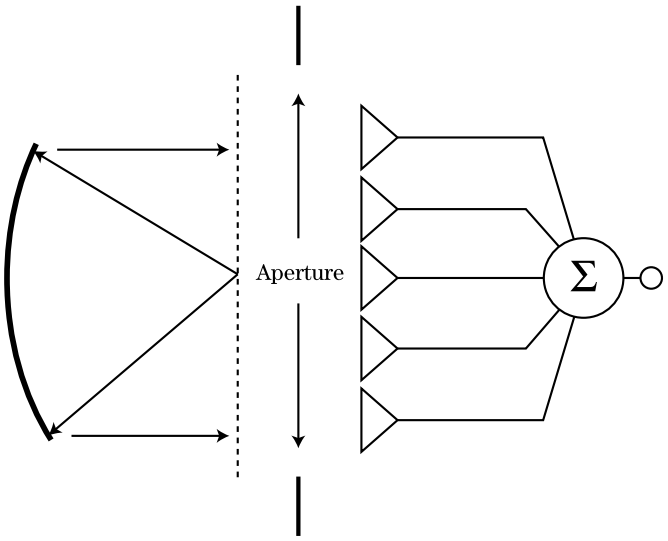

FIGURE 9-5 ■ The aperture for a reflector and array antenna.

Figure 9-6 shows uniform and low sidelobe aperture tapers and their resulting far-field radiation patterns. A mathematical function developed by Taylor provides a desirable combination of adjustable sidelobe control and minimal directivity loss [4,5]. Table 9-1 contains the aperture efficiency η_a and beamwidth factor α for several peak sidelobe levels when the Taylor function is applied to a linear array.

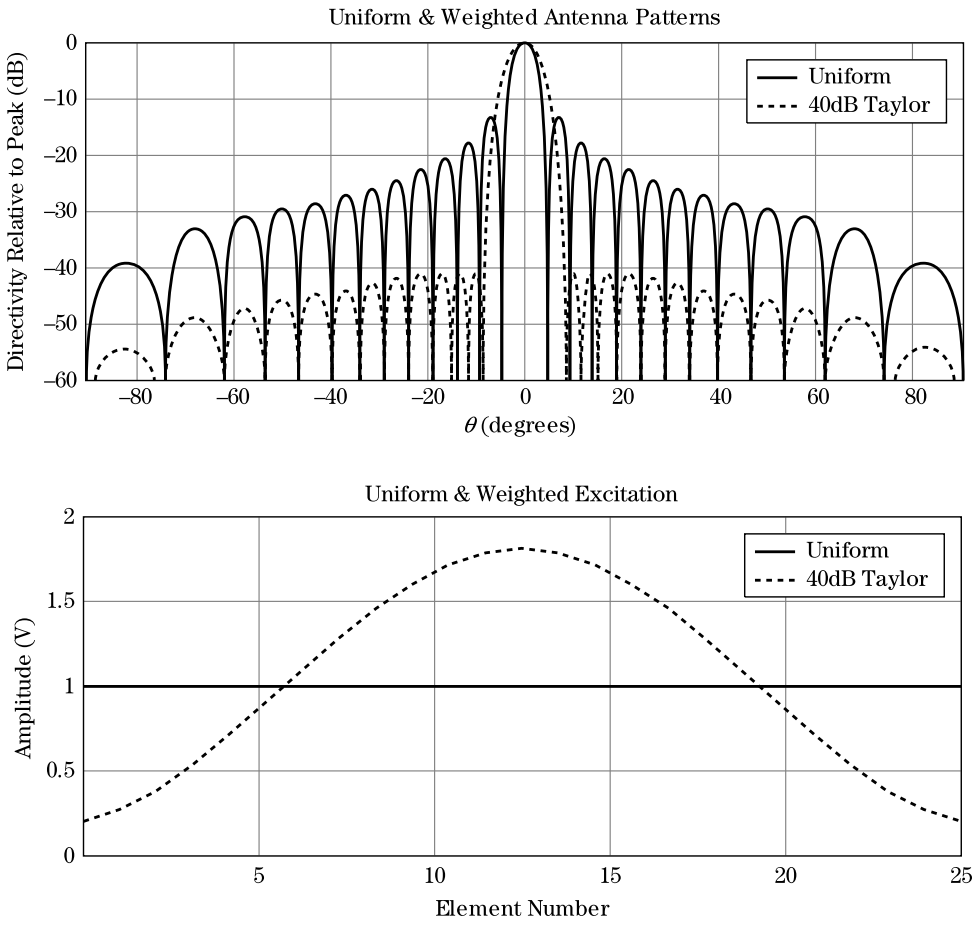

FIGURE 9-6 ■ Radiation patterns resulting from uniform and low sidelobe aperture tapers.

TABLE 9-1 ■ Aperture Efficiency and Beamwidth Factor Values for Different Taylor Distributions

Sidelobe Level (dB)	Beamwidth Factor (α)	Aperture Efficiency (η_a) dB
−13	0.88	0.0
−20	0.98	−0.22
−25	1.05	−0.46
−30	1.12	−0.70
−35	1.18	−0.95
−40	1.25	−1.18
−45	1.30	−1.39

Radar antennas are often rectangular apertures. In this case, independent Taylor tapers can be applied along the width and height of the aperture, resulting in different sidelobe levels for the azimuth and elevation radiation patterns. The beamwidth factor will then be different for the azimuth and elevation patterns, and the aperture efficiency will be the product of the horizontal and vertical efficiencies.

Taylor aperture tapers can be computed to provide arbitrarily low sidelobes, but it is very difficult to obtain first sidelobes below −40 dB in a real antenna system. This is because the ideal taper is never achieved due to errors caused by imperfections in antenna components, manufacturing tolerances, thermal effects, antenna alignment, and many other factors. Analysis of error effects is complex, is dependent on the specific type of antenna, and is treated in detail in the literature [6]. Herein, these effects are briefly discussed to illustrate how errors can affect the antenna's performance.

Aperture taper errors are typically treated as random deviations in amplitude and phase from the ideal taper function. Phase errors are typically harder to control and more destructive than amplitude errors. If there are no amplitude errors and the phase errors are uncorrelated from point to point throughout the aperture, their effect on maximum directivity can be expressed as [5]

$$\frac{D_e}{D_0} = \exp(-\delta_{rms}^2) \tag{9.8}$$

where D_0 is the maximum directivity of the antenna without errors, D_e is the maximum directivity of the antenna with errors, and δ_{rms} is the root mean square (rms) phase error in radians.

Equation (9.8) expresses the reduction of maximum directivity due to random phase errors in the aperture. This lost directivity represents power that will be scattered into the sidelobe region and will increase the average sidelobe level as described in equation (9.7). A phase error of 5° represents 5/360 or 1/72-nd of a wavelength of misalignment. At 10 GHz, this will be only 0.42 mm. Figure 9-7 shows the effect of phase errors on the directivity pattern. The 5° phase error causes significant degradation of the sidelobes.

The error analysis in Figure 9-7 treats only one type of error that can degrade an antenna's performance. There are additional sources of both amplitude and phase errors that are correlated across the aperture in different ways. These errors are best treated in computer simulations in which all errors are applied across the aperture with the proper statistics and correlation intervals. Simulations can be used to compute the far-field radiation pattern with errors added to the ideal taper to determine the combined effect. Since errors are treated as random variables, only one draw of random errors can be simulated

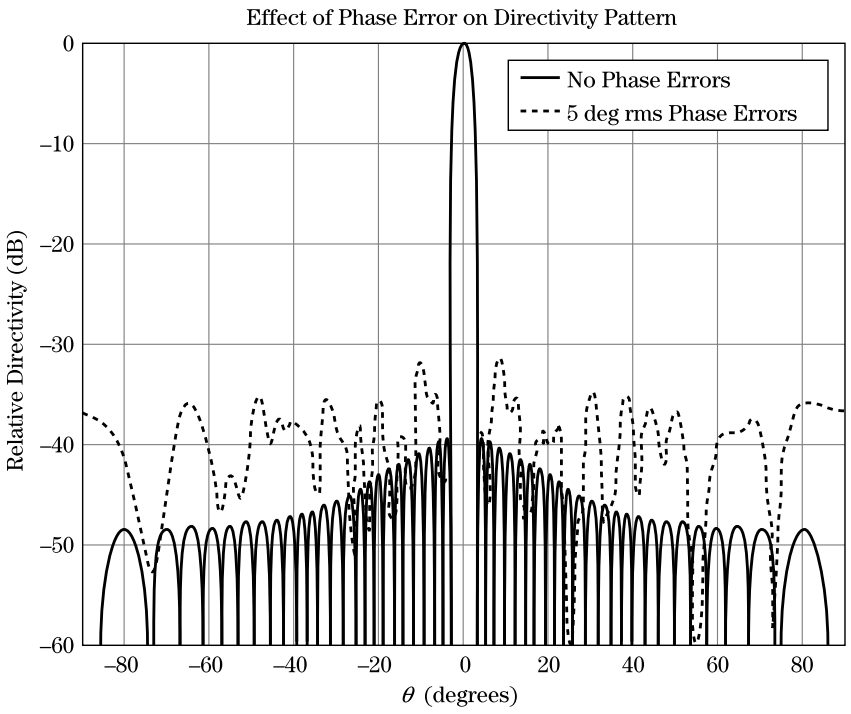

FIGURE 9-7 ■ Radiation pattern with and without random phase errors.

at a time. Therefore, the simulation should be run many times with the random number generators reseeded to get the proper statistical effects on the radiation patterns. For this reason the sidelobe metrics discussed in section 9.2 are often calculated based on the mean response of a Monte Carlo simulation that includes random errors.

9.4 | EFFECT OF THE ANTENNA ON RADAR PERFORMANCE

The antenna system has a significant impact on the overall radar performance. For instance, the radar "sees" the world through the antenna, which means a target can be detected only if it is located within the antenna's field of view (FOV). The field of view is defined as the angular region over which the main beam can be scanned. Depending on the type of antenna, the main beam can be moved throughout the field of view either by mechanically rotating the antenna or by electrically steering the beam, which will be discussed later in this chapter. In either case, the radar detection region is limited by the antenna's field of view.

The maximum range at which the radar can detect a target is highly dependent upon the antenna system. The maximum detectable range for a target of a given radar cross-section (RCS) σ is obtained from the radar range equation (see chapters 1 and 2) by determining the minimum detectable signal power $P_{\min}$ and then solving for the range at which that signal level is obtained, giving

$$R_{\max} = \left[\frac{P_t G^2 \lambda^2 \sigma}{(4\pi)^3 L_s P_{\min}} \right]^{1/4} \tag{9.9}$$

where the losses in the radar are combined into the term L_s. Note that the antenna gain is squared in this equation because the signal is transmitted and received by the same antenna. It is common for the gain to be different on transmit (G_t) and receive (G_r) due to different aperture weights, in which case G^2 is replaced by $G_t G_r$.

The ability of a radar system to resolve targets in range is inversely proportional to the system's instantaneous bandwidth. The minimum resolvable range for a compressed waveform is

$$\Delta R = \frac{c}{2B} \tag{9.10}$$

where c is the speed of light (3×10^8 m/s) and B is the radar's instantaneous bandwidth in hertz. The instantaneous bandwidth of a radar is often limited by the bandwidth of the antenna. It will be shown in section 9.7 that the instantaneous bandwidth of a phased array antenna is limited by the aperture size and the maximum electronic scan angle.

Most radar systems will either search for targets or track targets. These operating modes have slightly different antenna requirements, so key design decisions such as frequency selection and aperture size must be made with the primary radar operating mode in mind. A radar system that has to perform both of these functions is usually a compromise; that is, the search performance and track performance will be inferior to a radar designed to operate in only one of these modes.

The version of the radar range equation for tracking given in equation (2.59) can be expressed in a simplified form using peak power instead of average power as

$$\frac{P_t A_e^2}{\lambda^2} = \frac{4\pi (SNR) N_0 B R^4}{\sigma} \tag{9.11}$$

where the noise spectral power density is $N_0 = kT_0F$ and system losses L_s have been ignored. Equation (9.11) shows that the radar resources required to track a target with cross-section σ, at range R, with a given signal-to-noise (SNR) ratio SNR, can be expressed in terms of the product of the radiated power and the effective aperture area squared divided by the wavelength squared. Division by λ^2 implies that the same radar performance can be achieved with less power by increasing the frequency. The fact that area is squared indicates that it is more beneficial to increase aperture size than to raise power. In addition, it will be seen shortly that angular accuracy for tracking radars improves as the wavelength decreases. For these reasons, tracking radars tend to operate at higher frequencies with electrically large (i.e., large in wavelengths) apertures and relatively low power.

Search radars must search a solid angular sector in a given period of time to perform their mission. As presented in equation (2.44), the search form of the radar equation is

$$P_{avg} A_e = \frac{(SNR) 4\pi N_o L R^4}{\sigma} \left(\frac{\Omega}{T_{fs}} \right) \tag{9.12}$$

This equation states that a certain power-aperture product ($P_{avg} A_e$) is required to search an angular sector Ω in T_{fs} seconds to detect targets of RCS σ at range R. Unlike the tracking range equation, wavelength is not present in the search equation, which provides the freedom to operate at lower frequencies without performance degradation.

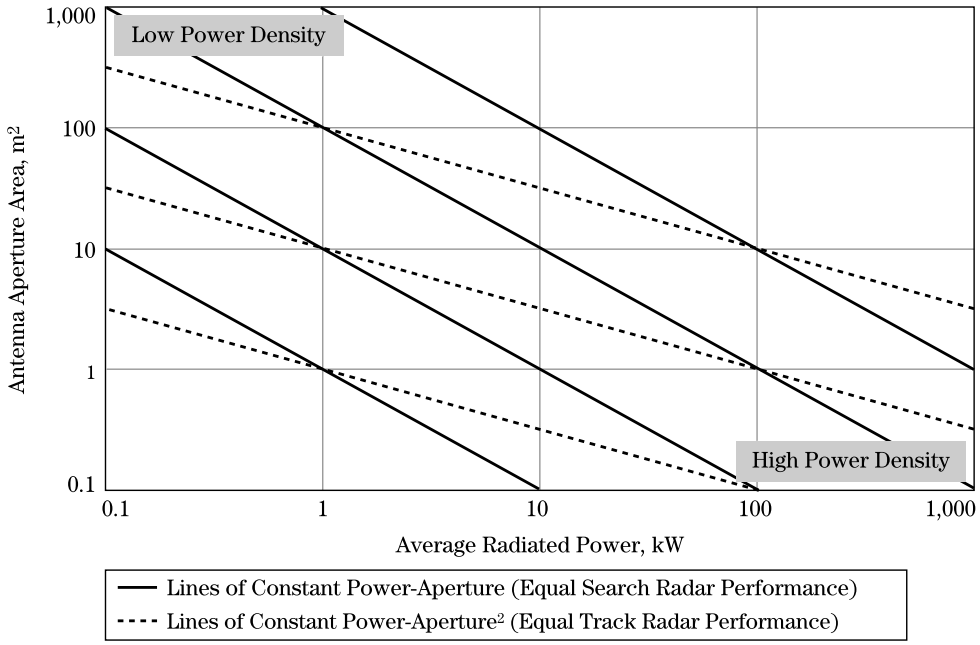

FIGURE 9-8 ■ Lines of constant track and search performance mapped onto the power-aperture space.

There are reasons lower frequencies are preferred for search radars. It is less expensive to make large apertures for lower frequencies since the tolerances, which are usually proportional to wavelength, can be relaxed. If the antenna is an array, the elements must be spaced less than a wavelength apart (see section 9.7) so fewer elements are required to fill a fixed-aperture area at lower frequencies. The beamwidth of an antenna with a fixed-aperture size is larger at lower frequencies so fewer beams are required to search the scan area in the required time. Finally, weather penetration is better at low frequencies due to reduced atmospheric attenuation.

Figure 9-8 displays the power-aperture space where the horizontal axis is average radiated power and the vertical axis is aperture area. The diagonal solid lines are lines of constant power-aperture product ($P_{avg}A_e$). As shown by equation (9.12), radar search capability will be the same for any point on a constant $P_{avg}A_e$ line. The dashed lines in Figure 9-8 are lines of constant $P_{avg}A_e^2$ for a fixed wavelength. According to equation (9.11), a radar will have the same tracking capability at any point on one of the constant $P_{avg}A_e^2$ lines. Figure 9-8 illustrates that power and aperture area can be traded to achieve the desired search or track performance. The optimum point on the curve will depend on prime power and spatial constraints imposed by the radar platform or the transportability requirements. For example, a radar in the nose of a fighter aircraft will typically have an aperture area of only 1 m^2, so it must increase power to achieve higher performance. This high-power density radar will operate in the lower right-hand corner of Figure 9-8. A space-based radar that collects solar energy to produce prime power will have a limited supply of transmit power; however, the aperture can be very large after deployment. This low-power density radar will operate in the upper left-hand corner of Figure 9-8. The power aperture requirement is a major driver on the modern radar antenna. Technologies and architectures to meet these requirements will be discussed in the following sections.

9.5 MONOPULSE

When searching for targets, it may be adequate to determine the target's angular location only to an accuracy equal to the antenna's 3 dB beamwidth. However, tracking usually requires a more accurate estimation of the target's angular position. The target's angular position can be determined more accurately than indicated by equation (9.4) by using monopulse [7]. In early systems additional accuracy was obtained by scanning the antenna beam over an angular area about the target and observing the amplitude modulation of the target return. These techniques, called conical-scan and sequential lobing [7], require several radar pulses to determine the target's position and are susceptible to errors caused by target RCS fluctuations. In addition, some jamming methods are effective against such tracking techniques.

The monopulse technique involves simultaneously generating and processing multiple closely spaced beams from the same antenna. This concept can most easily be described by considering two overlapping beams symmetrically offset from antenna normal, as shown in Figure 9-9. If the two beams are added together, an on-axis beam is formed that is commonly referred to as the sum beam (Σ). If the two beams are subtracted, the resulting pattern will have a positive lobe on one side of the axis, a negative lobe (*i.e.*, a lobe 180° out of phase) on the other, and a null that occurs on axis. This beam is referred to as the difference or delta beam (Δ).

To improve the tracking ability of a radar system, monopulse antennas create a signal proportional to the displacement of the target from the center of the Σ beam by comparing the outputs of the Σ and Δ beams. The monopulse error signal

$$v_{error}(\theta) = \frac{|\Delta(\theta)|}{|\Sigma(\theta)|}\cos\beta \tag{9.13}$$

is a function of the target's angle θ with respect to the antenna boresight and the phase angle β between the Σ and Δ beam outputs, which is designed to be nearly 0° or 180°,

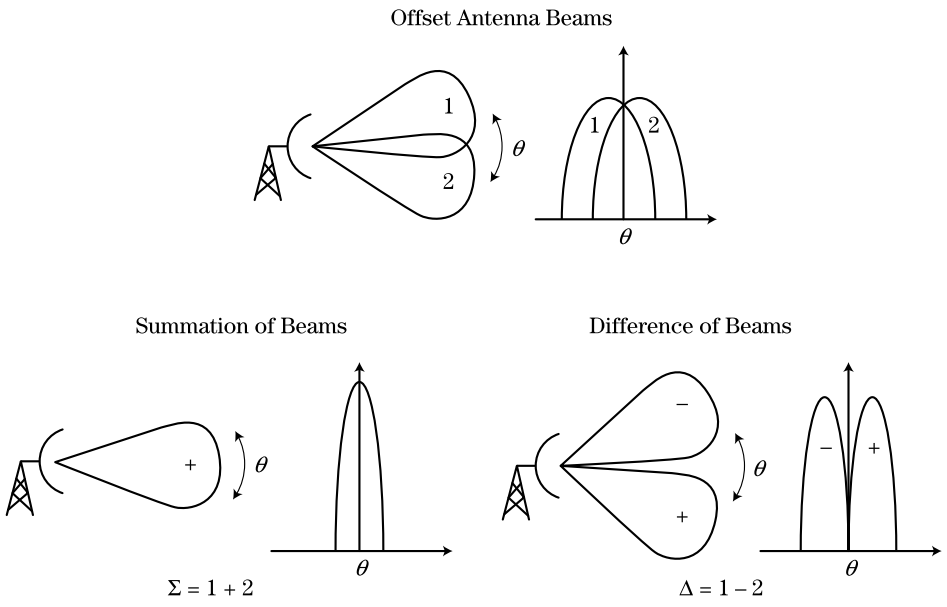

FIGURE 9-9 ■ A sum and delta beam can be formed by adding and subtracting overlapping antenna beams.

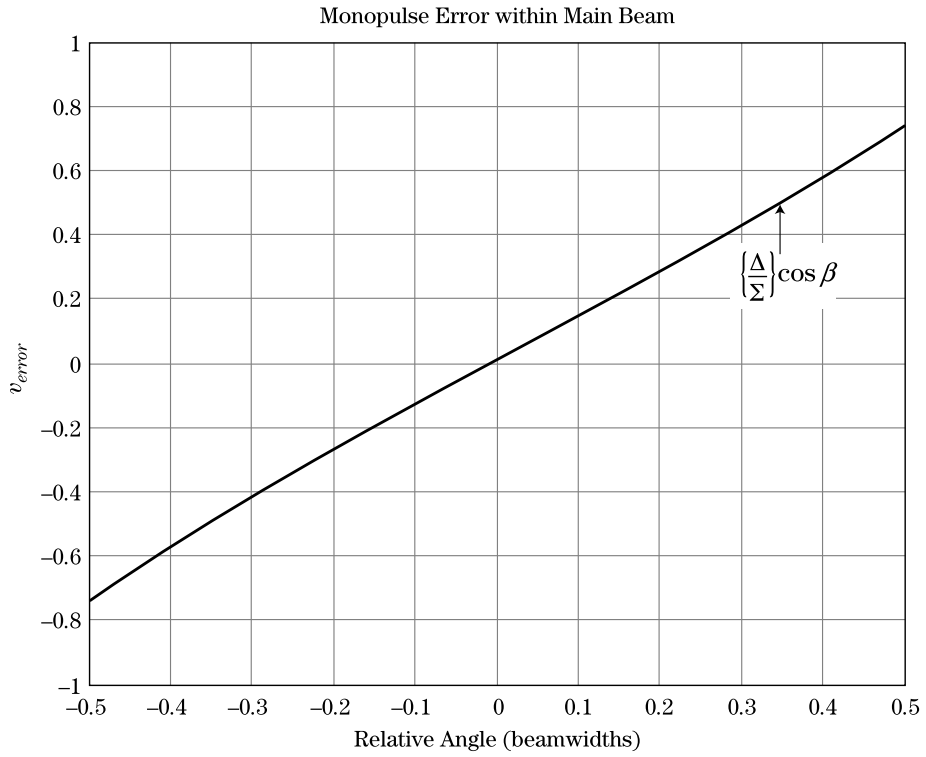

FIGURE 9-10 ■ The monopulse error signal is a ratio of the delta beam over the sum beam and is linear within the 3 dB beamwidth.

depending on from which side of center the target signal is entering. The angle θ is often normalized by the antenna beamwidth for convenience.

A typical error signal v_{error} is plotted in Figure 9-10 and is seen to be fairly linear between the 3 dB limits of the Σ beam. This error signal can be used to estimate the target's position within the Σ beam. The slope of the curve in Figure 9-10 is called the monopulse error slope k_m. With monopulse, the target's position can be measured in one pulse. Since the Δ beam is normalized by the Σ beam on each pulse, target RCS fluctuation will not create angle position errors beyond those created by changes in the SNR. The angular precision (standard deviation of angle error) that can be achieved using monopulse [7] is

$$\Delta\theta = \frac{\theta_3}{k_m\sqrt{2SNR}}\sqrt{1+\left(\frac{k_m\theta}{\theta_3}\right)^2} \tag{9.14}$$

where the monopulse error slope is k_m, and the target angle relative to the antenna normal is θ.

If a monopulse array with low sidelobes is required, a Taylor function can be used to generate the Σ pattern aperture taper, and a Bayliss [8] function can be used to generate the Δ pattern aperture taper. The Bayliss function is derived from the Taylor function and provides good sidelobe control for the Δ pattern while minimizing gain loss and beam broadening. The magnitudes of the Δ and Σ beams, using -40 dB Taylor and Bayliss functions, are shown in Figure 9-11.

The radar must transmit with the Σ pattern to put maximum power on the target and simultaneously receive with the Δ and Σ patterns. It is usually necessary to measure the target's position in both azimuth and elevation, so the previously described procedure must be performed in two dimensions. This requires a receive Σ beam and a receive Δ beam

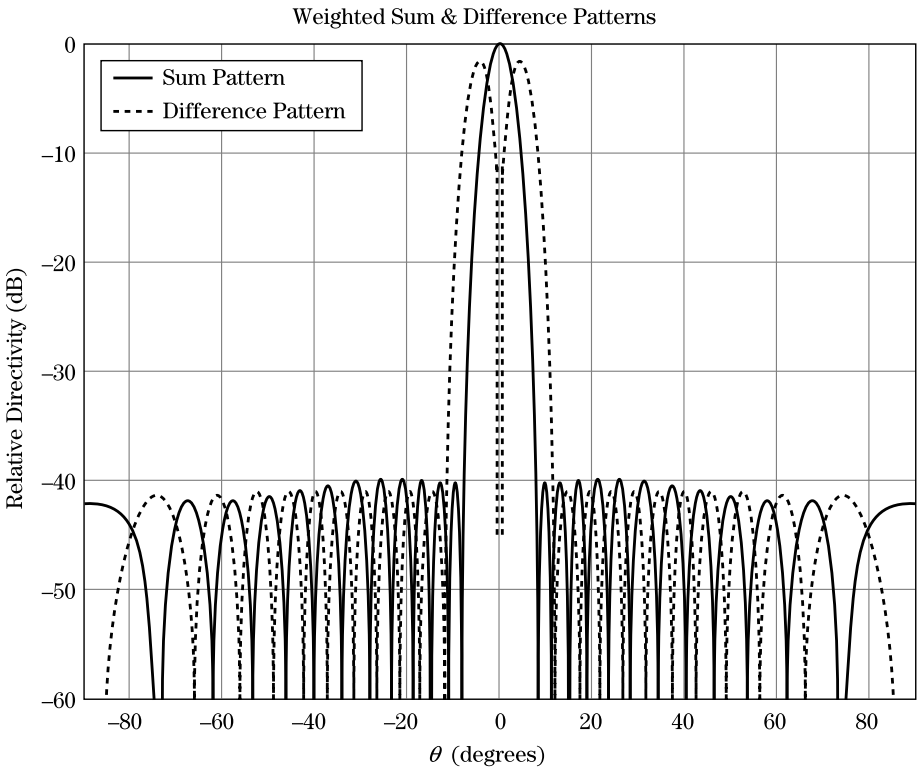

FIGURE 9-11 ■ Low sidelobe sum and delta patterns created with Taylor and Bayliss distributions.

in both the azimuth and elevation planes. Therefore, the monopulse radar requires at least three receive channels and a relatively complex antenna feed network.

9.6 REFLECTOR ANTENNAS

Mechanically positioned reflector antennas have been used in radar systems since the 1950s [9]. Today, nearly 60 years later, reflectors are still used for low-cost applications that require very high directivity with limited to no beam scanning. Most modern radar systems use phased array antennas for reasons discussed in section 9.7; nevertheless, reflectors can still be found in many radar systems. This section provides a brief introduction to the reflector antenna.

The most common reflector antenna is the parabolic reflector, which is shown in Figure 9-12. This antenna is formed by rotating a two-dimensional parabola about its

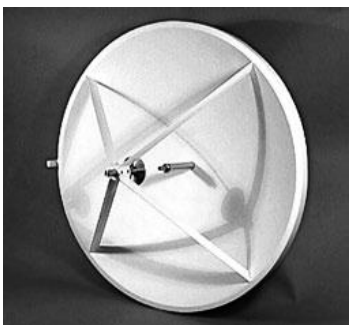

FIGURE 9-12 ■ Cassegrain reflector antenna developed by Quinstar Technology, Inc. (Used with permission.)

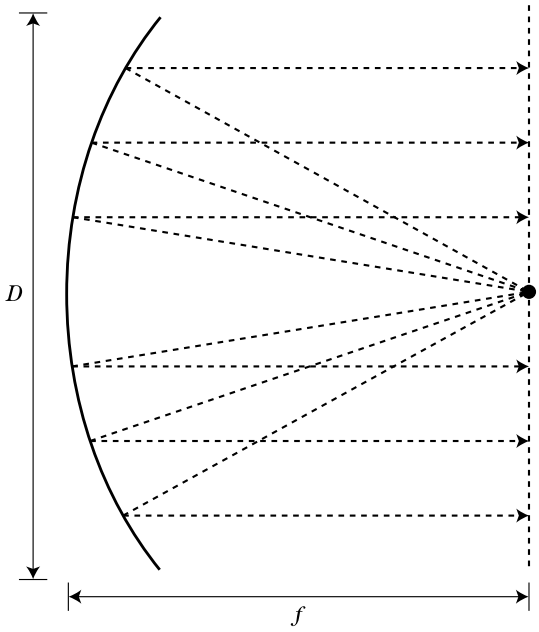

FIGURE 9-13 ■ For a parabolic reflector, all rays travel the same distance from the feed to the aperture plane.

focal axis. Geometric optics analysis (e.g., ray tracing) is a convenient way to illustrate the operation of a parabolic reflector antenna. Rays emanating from the feed point at the focus of the parabola will bounce off the parabolic reflector and travel, in parallel, to the aperture plane of the reflector. As shown in Figure 9-13, each ray will travel the same distance to the aperture plane, no matter which path is taken. Therefore, the spherically diverging wave emanating from the feed point will be collimated, or converted into a plane wave radiating perpendicular to the parabolas axis of rotation.

Conversely, if a plane wave is incident on the parabolic reflector along the axis of rotation, the energy in the plane wave will be coherently summed at the feed point. In a real, finite-sized reflector antenna, energy is concentrated to a spot located at the focal point of the parabola. A small feed antenna such as a pyramidal or conical horn is placed over the focal spot, as shown in Figure 9-14, and is connected to the radar transmitter and receiver through a circulator. The directivity pattern of the feed horn provides the aperture taper for the reflector; consequently, it is difficult to create the ideal Taylor tapers as discussed in section 9.3. If the feed pattern is too wide, significant energy will spill over (i.e., not intersect) the reflector and be wasted. On the other hand, if the feed pattern is too narrow the aperture will be under-illuminated and the aperture efficiency η_a will be reduced. The feed that provides the best compromise between spillover and aperture efficiency is one in which the -10 to -12 dB points of the feed pattern illuminate the edges of the reflector [10]. The angle to the reflector edge can be expressed in terms of the reflector diameter D and focal length f.

$$\theta_{edge} = 2\tan^{-1}\left(\frac{D}{4f}\right) \tag{9.15}$$

The focal length to diameter (f/D) ratio is an important design parameter for reflector antennas used in radar applications. This ratio is primarily determined by the curvature rate of the dish because the feed is fixed at the reflector's focal point. For example, a reflector with no curvature will have an (f/D) ratio of infinity. Reflector antennas are commonly designed to have (f/D) ratios between 0.25 and 0.5. A reflector with a high curvature

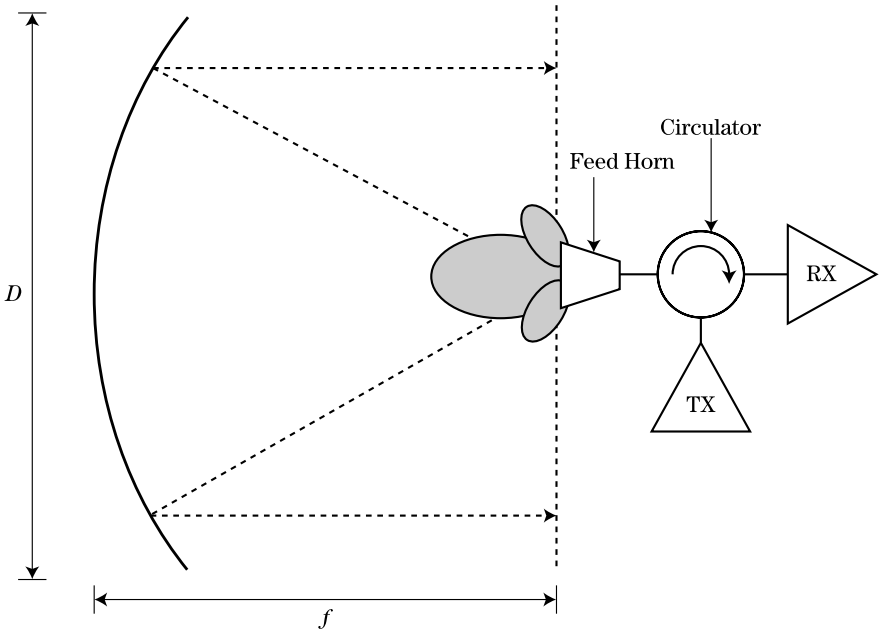

FIGURE 9-14 ■ The feed horn for a reflector antenna is sized to provide the desired aperture illumination on the reflector surface.

rate, and therefore a low value of (f/D), will suffer from polarization distortion and poor off-axis beam performance [6]. As the (f/D) ratio increases, the angle θ_{edge} will decrease, requiring a larger, more directive feed horn to provide a given aperture illumination. A large (f/D) requires that the feed be supported by long struts that are sometimes difficult to keep mechanically stable. The waveguide that connects the feed to the radar must run along one of these struts. This creates a long path between the transmitter and the feed, causing excessive losses. In addition, the feed and struts create a blockage to the antenna's aperture, which results in a gain loss and increases the sidelobe levels. This problem is exacerbated if the system is dual polarized, requiring multiple feed horns and multiple waveguide runs.

One way to alleviate the mechanical problems associated with a high (f/D) is to use a dual-reflector antenna, as shown in Figure 9-15. Here, the feed illuminates a small

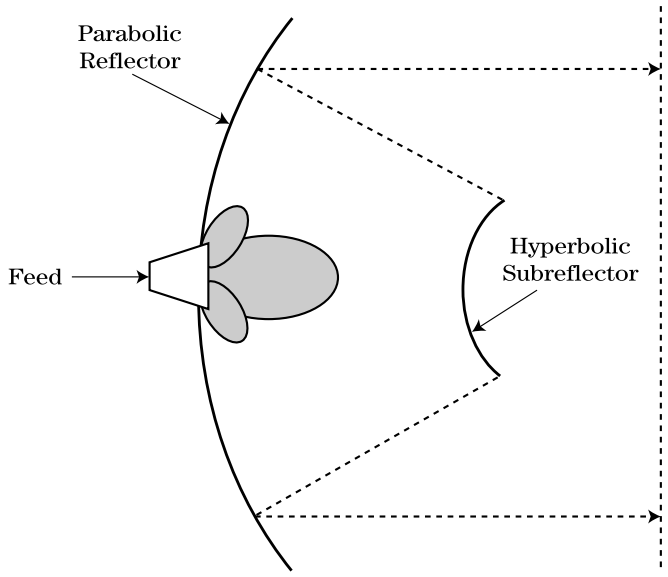

FIGURE 9-15 ■ Using a subreflector creates a long effective f/D in much less space.

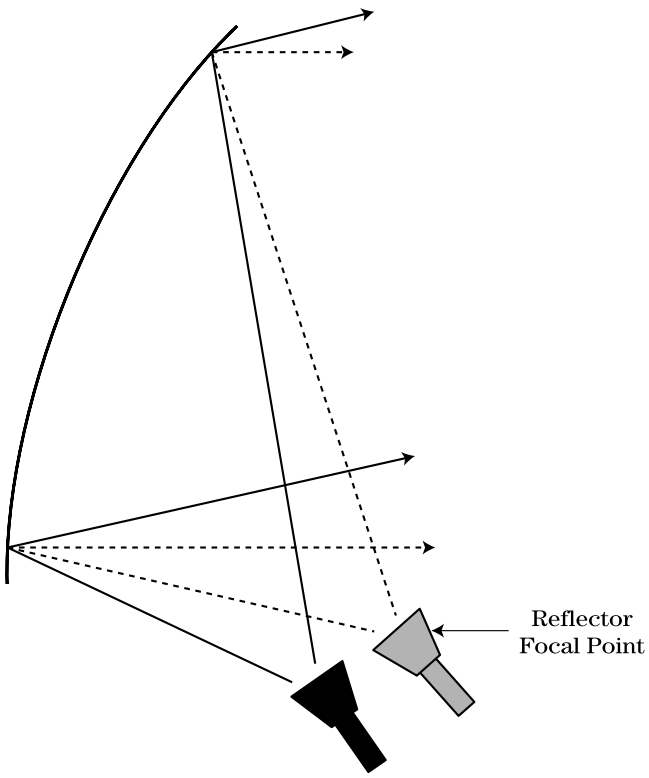

FIGURE 9-16 ■ The feed horn can be offset to eliminate blockage. Moving the horn from the focal point results in a limited amount of beam scanning.

hyperbolic subreflector with one of its foci located at the focus of the parabola [1]. This is called a *Cassegrain* configuration. This folded configuration provides an effectively long (f/D) reflector system in much less space and allows the feed waveguide to be brought in behind the reflector. The subreflector does create additional blockage of the reflector's aperture; however, the dual reflector system provides additional degrees of freedom for generating aperture tapers.

Blockage can be reduced or eliminated by using an offset or cut parabola in which the main reflector is made from a section of a parabola that is offset from the axis of rotation. From Figure 9-16 it can be seen that the focus of the parabola is now below the reflector and the radiated plane wave energy will not be blocked by the feed. The major drawback of this configuration is that the symmetry required for good monopulse performance is lost. This offset configuration is used for some search radars that do not require monopulse.

Reflector antennas can form multiple beams, or provide a limited amount of beam scanning, without mechanical motion of the reflector by displacing the feed horn from the parabola's focal point, as illustrated in Figure 9-16. However, if this method is used to scan the beam more than a few beamwidths, the resulting pattern will be severely distorted due to defocusing.

Search radars that mechanically rotate in azimuth sometimes use this limited scanning feature to form multiple elevation beams or to shape the elevation beam. If it is necessary to determine only the target's position in azimuth and range, the signals from multiple feeds can be combined to shape the elevation beam so it covers the required elevation angular area (i.e., 0° to 30°). If the target's elevation position also is needed, the radar input/output can be switched between multiple feeds to raster-scan the beam in elevation.

Reflector-based tracking radars use monopulse to enhance tracking accuracy. Sum and difference patterns are formed in the feed system by using multiple feeds displaced off the focal point to create the squinted beams and by combining them in a hybrid network or by using feed horns that can create multiple waveguide modes to form the multiple squinted beams [6].

9.7 PHASED ARRAY ANTENNAS

Phased arrays have become perhaps the most commonly used antenna in modern military radar systems. The reasons for this are plentiful. First, phased arrays provide high reliability, high bandwidth, and excellent sidelobe control. Second, there are certain applications for which phased arrays are uniquely qualified: phased arrays are ideal for stealth applications because they have no moving parts; they are ideal for airborne applications because they can electronically steer to extreme angles while maintaining a low profile, hence minimizing aircraft drag; and they are ideal for ground radar systems, which in some cases are too large for mechanical rotation, let alone rapid beam scanning. Finally, phased arrays have remarkable electronic beam agility that enables multiple functions to be performed nearly simultaneously by a single radar. Figure 9-17 is an example of a modern phased array, in this case in the nose of a fighter aircraft.

The largest disadvantage to the phased array antenna is cost. Phased arrays cost many times more than a reflector with the same gain; however, this cost gap has been decreasing. Phased array cost promises to decrease even further when technologies such as micro-electro-mechanical systems (MEMs) phase shifters and silicon-germanium (SiGe) mixed circuits replace some of the more expensive phased array components [11–13]. Nevertheless, the increased functionality of the phased array often justifies the additional cost.

9.7.1 The Array Factor

The basic concept of an array antenna was introduced in section 9.2. Essentially, an array is nothing more than collection of antennas that operates as a single unit. The individual antennas, often referred to as elements, are usually identical and uniformly

FIGURE 9-17 ■ AN/APG-81 – F-35 active electronically scanned array (AESA) radar. (Courtesy of Northrop Grumman Electronic Systems. Used with permission.)

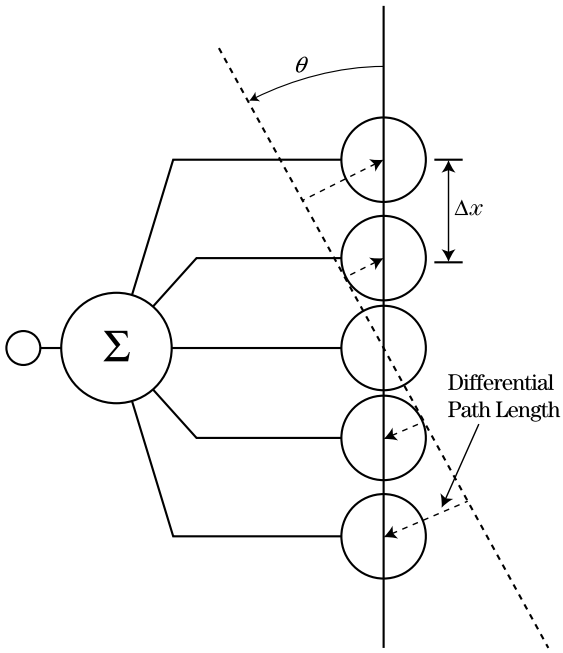

FIGURE 9-18 ■ A plane wave from angle θ intersecting with a five-element array.

spaced. Figure 9-18 shows a plane wave incident on a linear array of isotropic radiating elements from an angle θ with respect to array normal.

In the example in Figure 9-18, the interelement spacing is Δx, so the differential path length that the plane wave must propagate between one element and the next is $\Delta x \sin\theta$. This differential path length results in a relative phase shift between the signals at each element of $-(2\pi/\lambda)\Delta x \sin\theta$. The voltage response of the array to the plane wave is the sum of the individual element voltage responses. Normalized by the number of elements N, this is

$$AF(\theta) = \frac{1}{N}\sum_{n=1}^{N} \exp\left[-j\left(\frac{2\pi}{\lambda} n\Delta x \sin\theta - \phi_n\right)\right] \tag{9.16}$$

where ϕ_n is the relative phase shift between the n-th element and the array summation point. This expression is referred to as the *array factor* (AF) and is the key to understanding phased array antennas. The total radiation pattern of a phased array is the product of the array factor and the individual element pattern. If the element is assumed to be an isotropic radiator, which has no angular dependence, then the array factor and the phased array radiation pattern will be equal.

If the path length from each element to the summation point is equal, or $\phi_n = 0^\circ$ for all n, the array factor will be maximum when the plane wave approaches from a direction normal to the array. This is confirmed in equation (9.16) where the array factor is maximum (equal to 1) when $\theta = 0^\circ$ and $\phi_n = 0^\circ$. As θ increases, the element signals will no longer have equal phases due to the differential path lengths and will therefore no longer combine in phase, causing the array factor to decrease. This process was described in section 9.2.2 and plotted in Figure 9-4.

It is often desirable for an array to have maximum directivity at a non-zero incidence angle of θ_s. When the n-th element is excited by a plane wave arriving from an angle θ_s the phase at that element, relative to the first element, will be $-(2\pi/\lambda)n\Delta x \sin\theta_s$. If the

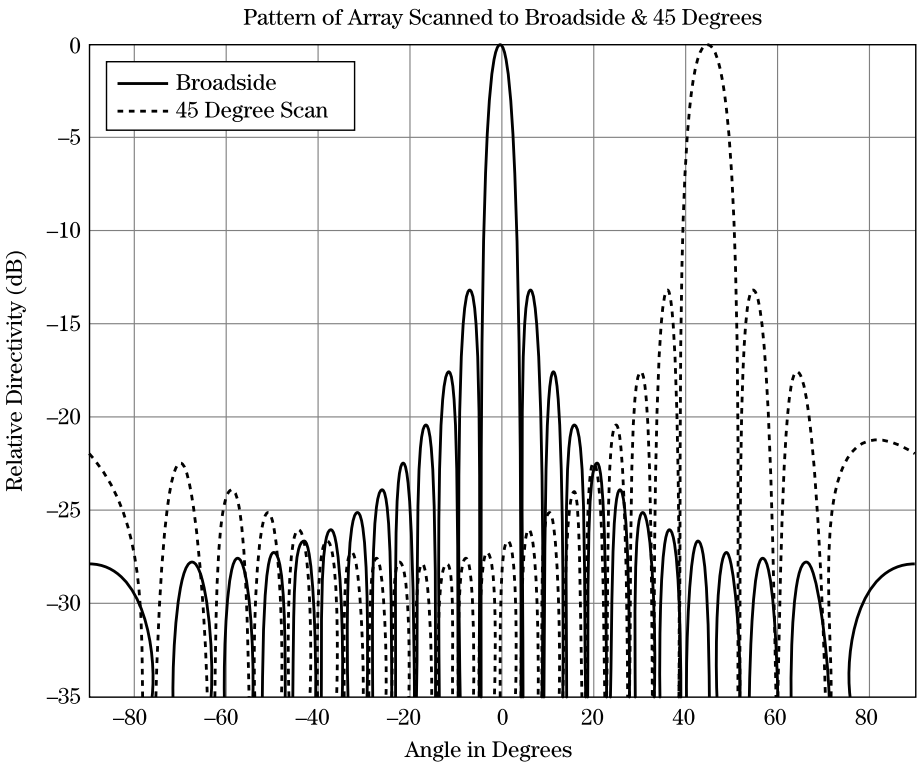

FIGURE 9-19 ■ Radiation pattern for an unsteered array and an array electronically scanned to 45°.

array elements are to coherently combine at this incidence angle, a progressive phase shift must be designed into the feed network that will essentially cancel the phase caused by the propagation delay. To accomplish this, the phase shift at element n must be

$$\phi_n = \frac{2\pi}{\lambda} n \cdot \Delta x \sin\theta_s \tag{9.17}$$

Substituting (9.17) into (9.16) yields

$$AF(\theta) = \frac{1}{N}\sum_{n=1}^{N} \exp\left[-j\frac{2\pi}{\lambda} n\Delta x(\sin\theta - \sin\theta_s)\right] \tag{9.18}$$

The array factor peak no longer occurs when $\theta = 0^\circ$ because the feed system is now adding a progressive phase shift to the response from each element. Instead, the array factor maximum will occur at $\theta = \theta_s$. Figure 9-19 shows the array factor when the array is unscanned ($\theta_s = 0^\circ$) and scanned to 45°($\theta_s = 45^\circ$).

By inserting the differential phase shift from equation (9.17) somewhere between the element and the summation point, the main beam can be electronically scanned to θ_s. But how is this phase shift inserted? The phase shift could be realized by adding physically longer path lengths between the elements and the summation point. The path length would need to be proportional to the desired phase delay; however, this method would be "hard-wired" and would work only at one scan angle. A smarter approach uses a device called a *phase shifter* that can dynamically change the phase delay from pulse to pulse.

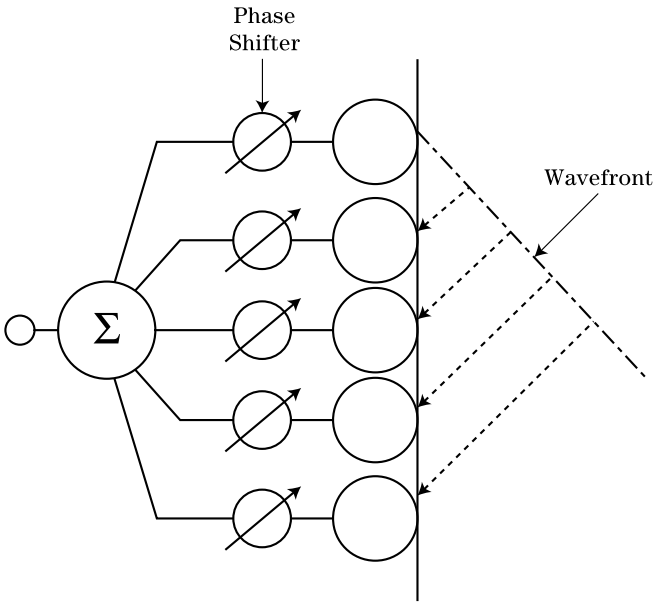

FIGURE 9-20 ■ Phase shifters can be inserted after the radiating elements to electronically scan the beam.

9.7.2 Phase Shifters

If a phase shifter is installed behind each of the radiating elements, as shown in Figure 9-20, then the array can be quickly resteered by simply adjusting the phase-shifter settings. The phase through each phase shifter will be set according to equation (9.17) for the desired scan angle. This dynamic electronic scanning capability of phased arrays makes them very attractive for modern radar applications. The antenna beam can be moved quickly in an arbitrary pattern; sequential scanning is not required of phased arrays.

Phase-shifter technology has been an energetic research area for the last 60 years, and an extensive discussion of these devices can be found in [10,14]. The discussion here will highlight key concepts that every radar engineer should understand. Figure 9-21 shows a simple switched line length phase shifter. This is commonly referred to as a 3-bit phase shifter because it has three line segments, each one-half the length of the next, that can be switched in and out to add phase shift. In this example the least significant bit causes a 45° phase delay. This leads to the first key concept, which is that phase shifters do not have arbitrarily fine phase resolution. Assume that a specific scan angle requires a phase shift of 63°. The phase shifter in Figure 9-21 would switch in its closest approximation, the 45° delay line, leaving an error of 18°. This error is referred to as a *phase quantization error* and is determined by the number of bits in the phase shifter.

Because each antenna element requires a different phase shift, the errors across the array will often appear to be random. Hence, these quantization errors are typically modeled as random errors, and, as discussed in section 9.3, they tend to increase the sidelobe

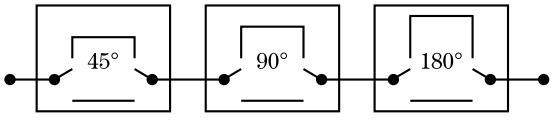

FIGURE 9-21 ■ Example of a 3-bit switched line length phase shifter.

TABLE 9-2 ■ Relationship among Phase-Shifter Bits, Phase Error, and Gain Loss

Number of Bits (N)	Least Significant Bit	RMS Phase Error	Gain Loss (dB)
2	90°	26°	0.65
3	45°	13°	0.15
4	22.5°	6.5°	0.04
5	11.25°	3.2°	0.01
6	5.625°	1.6°	0.00

levels of the radiation pattern. As the number of phase-shifter bits increases, the quantization error will decrease and the antenna sidelobe performance will improve. Also, as the sidelobe energy decreases the directivity will become larger. This relationship is shown in Table 9-2. The actual gain loss depends on the antenna size, shape, and aperture weighting, but the values in the fourth column are representative. On the other hand, insertion loss through the phase shifter will also increase with the number of bits. Therefore, it is not always beneficial to use the highest-resolution phase shifter available.

The second key concept is that phase shifters are not ideal for wideband radar applications because the required phase delay for a scanned beam is frequency dependent, as evidenced by the appearance of λ in equation (9.17). Thus, for a chirp waveform the antenna will have the right phase shift only at one frequency in the waveform. Section 9.7.6 will discuss methods to overcome this problem.

9.7.3 Grating Lobes

An examination of equation (9.18) reveals that it may be possible for more than one AF maximum to occur within the range of $-90^\circ \leq \theta \leq 90^\circ$. Specifically, maxima will occur for values of θ that satisfy

$$\frac{\Delta x}{\lambda}(\sin\theta - \sin\theta_s) = 0, \pm 1, \pm 2, \ldots \tag{9.19}$$

The maxima that corresponds to a value of zero on the right-hand side of equation (9.19) is the intended beam and has its peak at $\theta = \theta_s$. The maxima corresponding to nonzero integers are called *grating lobes* and have their peaks at values of θ other than θ_s. Grating lobes are usually undesirable for radar applications because they can induce angular ambiguities and hinder the radar's ability to locate targets. The radar may mistakenly report that a target is in the main lobe when in reality it was an object, such as clutter or a jammer, in the grating lobe.

The solid pattern in Figure 9-22 shows an array factor where the elements are spaced one wavelength apart ($\Delta x = \lambda$) and the main beam is unscanned ($\theta_s = 0^\circ$). Since the elements are spaced one wavelength apart, a plane wave incident from either end of the array ($\theta = \pm 90^\circ$) will travel exactly one wavelength between adjacent elements, and therefore the element signals will combine in phase. The lobes at $\pm 90^\circ$, or $\sin\theta = \pm 1$, are the grating lobes.

As an aside, it should be noted that the array factor in Figure 9-22 is plotted as a function of $\sin\theta$ instead of θ. Since $\sin(90^\circ) = 1$ and $\sin(-90^\circ) = -1$, all angles in the antenna's forward hemisphere are mapped onto the $\sin\theta$ axis between -1 and 1. This coordinate system is referred to as *sine space* and is commonly used because it stresses the periodicity of the array factor.

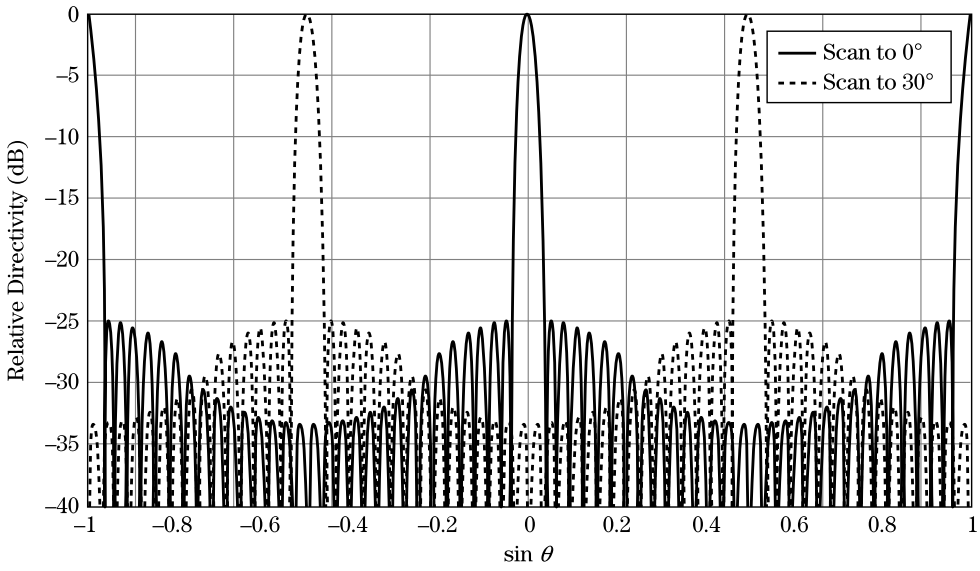

FIGURE 9-22 ■ Antenna pattern with grating lobes for a scanned and unscanned array with one wavelength element spacing.

The dashed pattern in Figure 9-22 shows the same array electronically scanned to 30° (a value of 0.5 in sine space). The grating lobe location has moved from −90° to −30°, which demonstrates that grating lobes scan with the main beam. The distance between the main lobe and the grating lobe is still one in the sine space coordinate system; hence, electronic scanning does not change the distance between the main lobe and the grating lobe.

Grating lobes can be prevented if Δx is made small enough. Equation 9.19 shows that the period between the grating lobes and the main beam is set by the element spacing in wavelengths. Specifically, in sine space, the array factor is periodic with period $\lambda/\Delta x$. Decreasing the element spacing with respect to the wavelength will push the grating lobes farther apart. Therefore, if it is required to scan the array to θ_s without grating lobes, the period of the array factor must be at least $1 + \sin\theta_s$, or

$$\Delta x \leq \frac{\lambda}{(1 + |\sin\theta_s|)} \tag{9.20}$$

According to equation (9.20), Δx must be less than 0.667λ if the array is to be scanned to 30° without a grating lobe. The solid line in Figure 9-23 shows a linear array scanned to 30° with an element spacing of $\Delta x = 0.667\lambda$. The grating lobe is located at $\sin\theta = -1$. For comparison the dashed line shows a similar array with an element spacing of λ. The grating lobe is now much closer at $\sin\theta = 0.5$. By using $\theta_s = \pm 90°$ in equation (9.20), it can be seen that an element spacing of $\lambda/2$ is adequate for any scan angle and is therefore commonly assumed.

For a given aperture size there is an important trade between the number of elements and grating lobes. Grating lobes are avoided by spacing elements close together, but this requires additional elements, additional electronics, and, ultimately, incurs additional cost. Therefore, a phased array designer will often use the maximum spacing allowed by equation (9.20). This avoids grating lobes while minimizing cost. Maximum spacing is calculated using the highest operational frequency and greatest scan angle.

The grating lobe discussion is this section was limited to linear arrays. For a discussion of preventing grating lobes in a two-dimensional array, see [15].

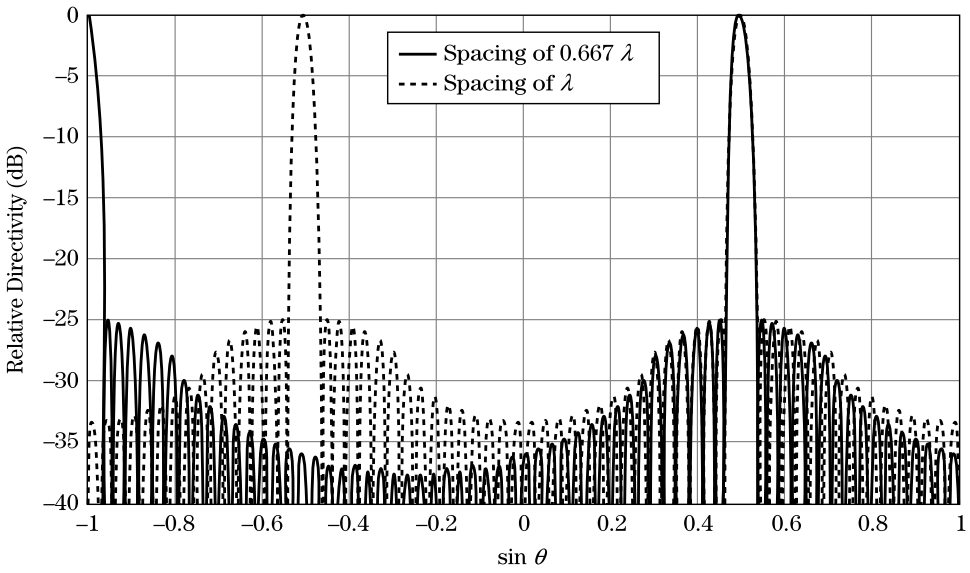

FIGURE 9-23 ■ Comparison between two arrays showing that grating lobes become less significant when the element spacing decreases.

9.7.4 Gain Loss

When a reflector antenna is mechanically scanned, the aperture and main beam are always pointing in the same direction, and the full antenna gain is realized at all scan angles. This is not the case with phased arrays. A negative byproduct of electronic scanning is gain loss. Gain loss is most significant at large scan angles and is caused by a decrease in the projected aperture of the array.

When a phased array is electronically scanned, the antenna does not move; hence, the projected aperture area in the direction of the main beam is reduced by $\cos\theta_s$. This is shown in Figure 9-24. Recall from equations (9.4) and (9.5) that the beamwidth and directivity are both related to the aperture size. If the aperture is reduced by $\cos\theta_s$ the directivity will be reduced by the same amount. The beamwidth is inversely proportional to aperture size and will be increased by a factor of $1/\cos\theta_s$. To illustrate this point further, consider a phased array scanned to 60°. At this scan angle the main beam will be twice

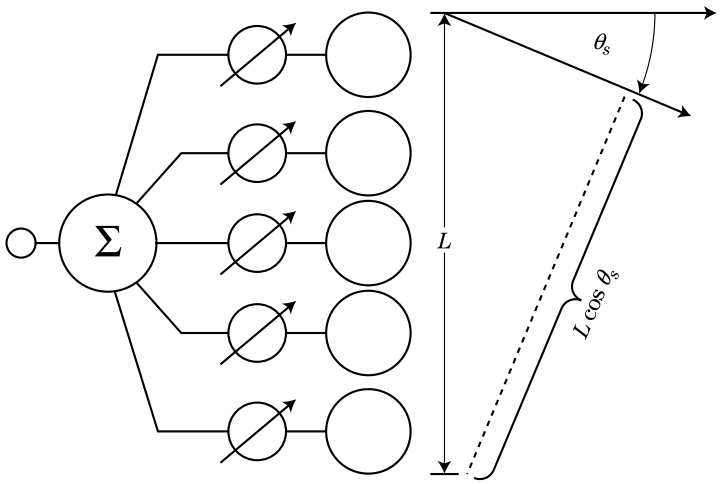

FIGURE 9-24 ■ The projected aperture of a phased array decreases with scan angle, resulting in beam broadening and a directivity loss.

as large as it is at broadside, and the directivity will be reduced by 3 dB. For monostatic radar the two-way loss at 60° will be 6 dB. This phenomenon usually limits the maximum practical scan angle of a phased array to ±60°.

As seen in equation (9.9), the maximum detection range of a radar is proportional to the antenna gain squared. Thus, at large scan angles, where gain loss is most significant, a phased array needs more sensitivity than a comparable mechanically scanned array.

Fortunately, several factors help mitigate the gain loss of a phased array. For a search radar, one of the loss terms (*scalloping loss*) is associated with the target not being at the peak of the beam at all times. Since the beam is widened at non-zero scan angles, for a constant separation of beam positions this scalloping loss is reduced, partially offsetting the gain loss. Most modern phased array systems have the ability to adapt the dwell time to compensate for gain loss. For near-normal beam positions, the dwell time can be reduced, and at far-out beam positions the dwell time can be lengthened to account for gain variation. For a track radar, the reduced gain and wider beamwidth will degrade track precision. For important threat targets, though, the dwell time can be extended to offset these effects.

9.7.5 The Array Element

So far the individual radiating elements that make up a phased array have been assumed to be fictitious isotropic radiators that do not impact the array's directivity pattern. In reality the array elements contribute significantly to the overall antenna performance. The element largely determines the array polarization as well as the impedance match and scan loss. Although the design of array elements is treated elsewhere [1–3] and is beyond the scope of this chapter, a few comments about array elements will be made.

First, combining the array factor from equation (9.18) with the element directivity pattern $E_e(\theta)$ yields

$$E(\theta) = E_e(\theta)AF(\theta) = \frac{E_e(\theta)}{N}\sum_N \exp\left[-j\frac{2\pi}{\lambda}n\Delta x(\sin\theta - \sin\theta_s)\right] \tag{9.21}$$

where $E(\theta)$ is the total antenna directivity pattern. Figure 9-25 shows an array with directive elements.

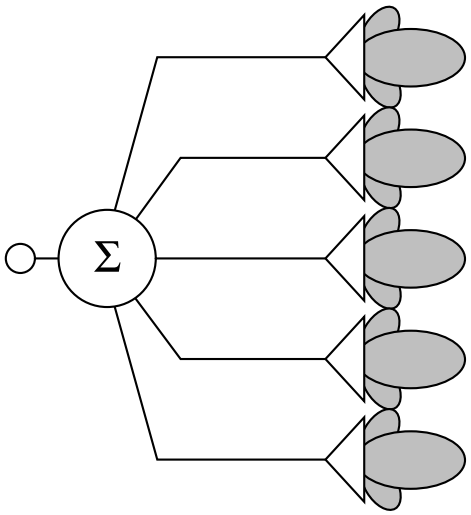

FIGURE 9-25 ■ Array elements are not isotropic and therefore have directivity.

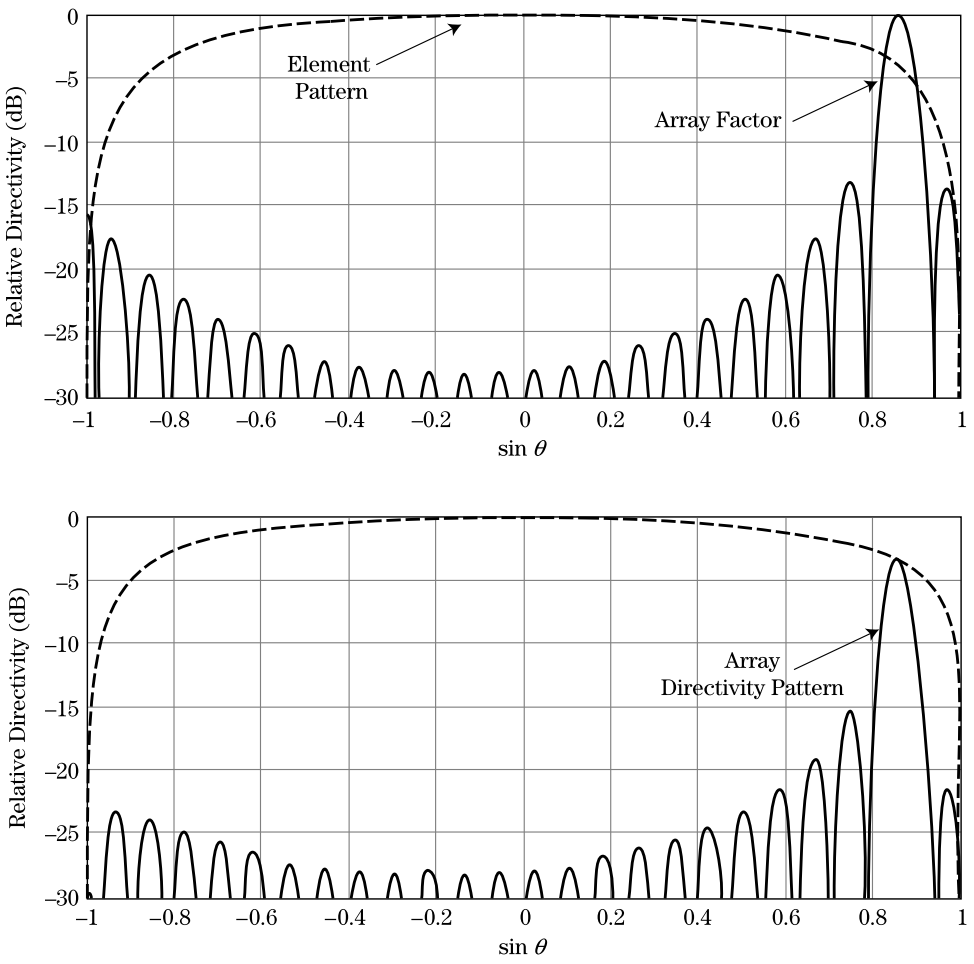

FIGURE 9-26 ■ The total antenna pattern of an array (lower plot) is the product of the array factor and the element pattern (upper plot).

According to equation (9.21) the directivity pattern of the array is the product of the array factor and the directivity pattern of a single array element. This is illustrated in Figure 9-26. When the array is electronically scanned, a phase shift is applied at each element, causing the array factor to electronically scan in the direction of θ_s, but the element pattern remains unchanged. Therefore, as the array scans it "looks" through a different part of the element pattern, and, as a result, the scanned main beam is weighted by the directivity of the element pattern at that scan angle. In an extreme scenario, if the element pattern has a null in the direction θ_s, then the array will be blind in this direction even though the array factor may be maximized. Thus, phased array gain loss is proportional to the directivity of the individual elements.

Antenna elements are usually designed such that the 3dB beamwidth is equal to the required array field of view (FOV). Therefore, $\cos\theta$ is a perfectly matched element pattern for an array with a maximum scan volume of 60°. The antenna element provides the impedance match between the feed system and free space for all scan angles and cannot be perfectly matched over all operating conditions. Elements are usually designed to have peak performance at broadside; thus, the match worsens with angle resulting in additional scan loss. For a full FOV (scan to $\pm°60$) radar, the element pattern is typically assumed to be $\cos^{1.5}(\theta)$ to account for this increased mismatch with scan angle. It is important

to reiterate that the element pattern gain loss accounts for the aperture projection loss discussed previously.

There is an assumption made in equation (9.21) that is valid only for large phased arrays. This assumption is that each element has the same directivity pattern. In fact, the characteristics of an element in the array environment (surrounded by other elements typically spaced one-half wavelength apart) are quite different from what they are for an isolated element of the same type. An element near the edge of the array will "see" a different environment from what an element near the center of the array sees and will therefore have a different radiation pattern. In a 3×3 planar array, eight elements are edge elements, and only one is surrounded by others. The assumption of identical patterns for all elements is not valid for this scenario. However, if the array has 100×100 elements, 396 elements are on the edge and 9,604 are embedded in the array environment, and the assumption is valid.

Finally, polarization is specified for almost all radar antennas. For mechanically scanned systems the polarization needs to be specified only at broadside. However, with a phased array the polarization requirement will be scan angle dependent because the array "sees" through different places in the element pattern as it scans and because the element polarization can change with angle. If the polarization of the element pattern at 60° is different than at broadside, which is likely, the polarization of the main beam of the full array will also be different at a 60° scan angle. The antenna element will often exhibit the desired polarization at broadside and deteriorating polarization purity with increasing scan angle.

9.7.6 Wideband Phased Arrays

Modern radars require large instantaneous bandwidths to resolve targets in range [9,10, Chapter 20]. Regrettably, a traditional phase shifter-based phased array cannot simultaneously support wideband waveforms and electronic scanning. The phase required at element n to electronically scan a beam to angle θ_s is frequency dependent, as was seen in equation (9.17). For narrowband waveforms this is not a problem because the phase shifter can be reprogrammed between pulses to compensate for frequency hopping and new scan angles. However, for wideband operation the phase shifter can be accurate only at one frequency within the wideband spectrum and this is usually chosen to be the center frequency. As will be shown, the result is a beam-pointing error proportional to the instantaneous bandwidth.

Equation (9.21) applies to single frequency operation where λ is constant. When the radar waveform has extended bandwidth, equation (9.21) becomes

$$E(\theta, \lambda) = \frac{E_e(\theta, \lambda)}{N} \sum_N \exp\left[-j2\pi n \Delta x \left(\frac{\sin\theta}{\lambda} - \frac{\sin\theta_s}{\lambda_0}\right)\right] \tag{9.22}$$

where λ is the wavelength of any spectral component of the waveform and λ_0 is the wavelength at the center frequency of the waveform where the phase-shifter setting is determined.

In equation (9.21) the argument of the exponential term is zero, and all of the elements combine coherently, when $\sin\theta = \sin\theta_s$. In equation (9.22), the argument of the exponential is zero when

$$\frac{\sin\theta}{\lambda} = \frac{\sin\theta_s}{\lambda_0} \tag{9.23}$$

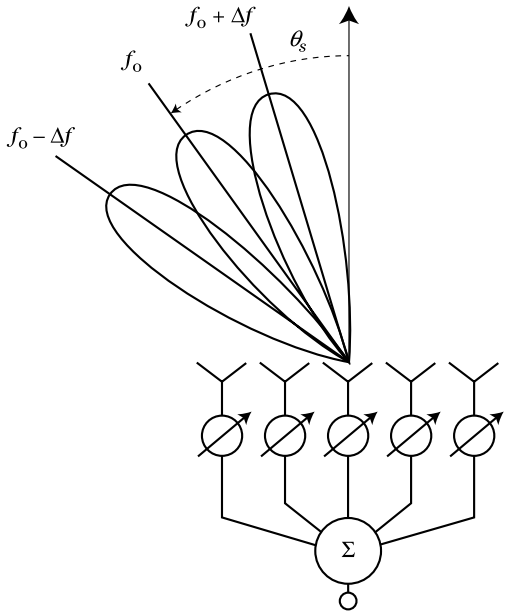

FIGURE 9-27 ■ A phase-shifter-based phased array will mispoint the beam during wideband operation for off-broadside scan angles.

From (9.23) it can be seen that a small change in frequency causes a mispointing error of

$$\Delta\theta = \frac{\Delta f}{f_0} \tan\theta_s \tag{9.24}$$

where the difference between the instantaneous frequency and the center frequency is Δf, and the resulting mispointing, or angular squint, is $\Delta\theta$. Therefore, every spectral component of the waveform will be scanned into a different direction centered about θ_s. This situation is depicted in Figure 9-27.

If it is determined that the radar can tolerate a beam squint of ±one-half of the 3 dB beamwidth, then $\Delta\theta$ can be set to $\theta_3/\cos\theta_s$ (remember the beam broadens by $1/\cos\theta_s$ with scanning), and the maximum tolerable instantaneous signal bandwidth in equation (9.24) becomes

$$B_i \equiv \left(\frac{\Delta f}{f_0}\right)_{\max} = \frac{\theta_3}{2\sin\theta_s} \tag{9.25}$$

where θ_3 is the 3 dB beamwidth in radians at broadside. The instantaneous bandwidth in equation (9.25) can be approximated with an engineering equation as

$$B_i\ (\%) \approx 2\theta_3\ (\text{degrees}) \tag{9.26}$$

where the instantaneous bandwidth B_i is expressed as a percentage, and the beamwidth has units of degrees. This simplified equation assumes a maximum scan angle of 60°. For example, an array with a 1° beamwidth can support only a 2% instantaneous bandwidth at a 60° scan angle. It is important to point out that this problem becomes exacerbated for large apertures that have smaller beamwidths. The mispointing angle does not change with aperture size; however, it becomes a larger percentage of the antenna beamwidth. Many modern radars have a beamwidth of 1° or less and require bandwidths of 10% or greater. In these cases, something must be done to overcome the limitation expressed in (9.26).

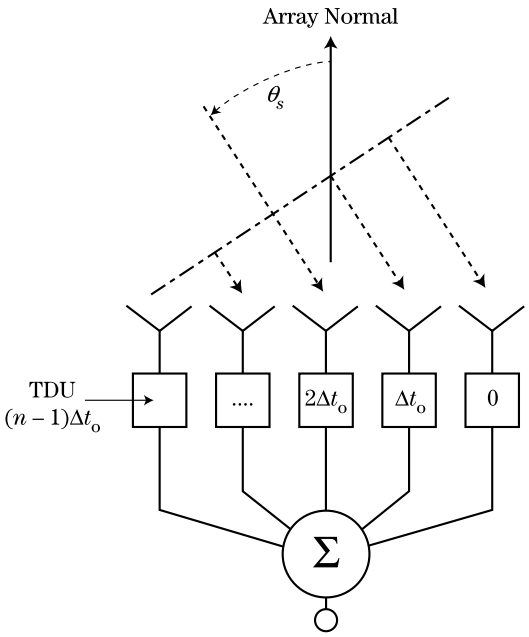

FIGURE 9-28 ■ The phase front of an off-axis plane wave will strike each element at a different time. The time of arrival difference is frequency independent. A TDU-based phased array is ideal for wideband operation.

One approach to improving bandwidth is to replace the phase shifters at each element with time delay units (TDUs). Instead of adjusting for the phase difference induced by the incident off-axis plane wave, the TDU will adjust for the difference in time of arrival at each element, as illustrated in Figure 9-28.

The differential time delay Δt at each element is

$$\Delta t_n = \frac{n\Delta x \sin\theta_s}{c} \tag{9.27}$$

which results in a phase shift of

$$\phi_n = 2\pi\,\Delta t_n f = \frac{2\pi}{\lambda} n\Delta x \sin\theta_s \tag{9.28}$$

Rewriting (9.22) for time delay scanning yields

$$E(\theta, \lambda) = \frac{E_e(\theta, \lambda)}{N} \sum_n \exp\left[-j\frac{2\pi}{\lambda} n\Delta x(\sin\theta - \sin\theta_s)\right] \tag{9.29}$$

By using TDUs instead of phase shifters, the phase shift at each element is automatically corrected for each spectral component and eliminates beam squinting. This is because, although each spectral component of the waveform travels a different distance in wavelengths to each element, all spectral components travel at the speed of light and therefore have equal time delay. The bandwidth problem would be solved if TDUs could be placed behind each antenna element. Unfortunately, with current technology TDUs are still too large and expensive to embed behind individual elements. Therefore, a compromise solution is gaining popularity in many large phased array systems.

The compromise solution is presented in Figure 9-29. The array is broken into small sections called subarrays, which will be discussed in section 9.8.3. Each subarray is sized to have a beamwidth determined by equation (9.25) and the desired bandwidth. Conventional phase shifters are used within the subarrays, and TDUs are used to provide time delay

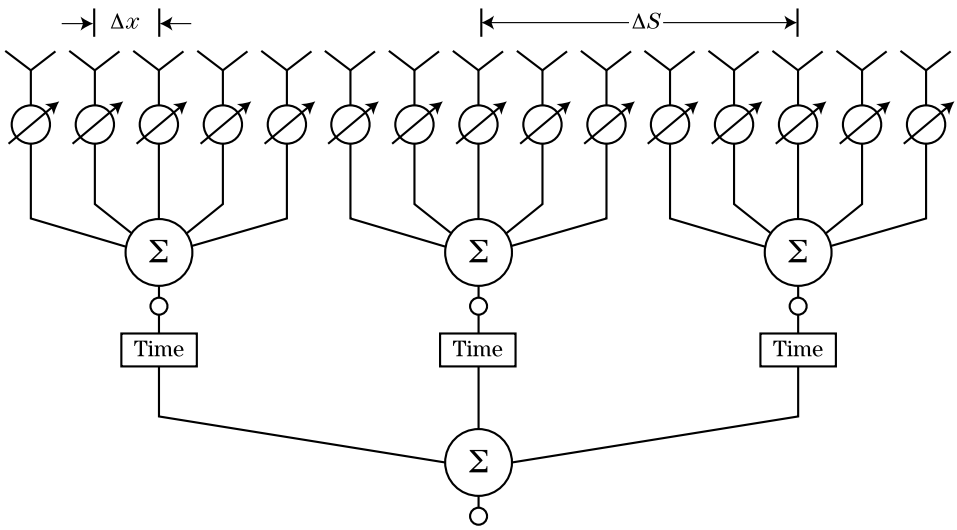

FIGURE 9-29 ■ The subarray architecture is often used for wideband operation with TDUs inserted behind each subarray.

between subarrays. The subarray pattern will squint according to equation (9.24) because it is scanned using phase. The subarray AF, which determines the location of the full-array main beam, operates according to (9.29) and will not mispoint with frequency. The resulting equation for the directivity pattern is

$$E(\theta,\lambda) = \frac{E_e(\theta,\lambda)}{MN} \tag{9.30}$$
$$= \sum_M \exp\left[-j\frac{2\pi}{\lambda}m\Delta S(\sin\theta - \sin\theta_s)\right] \sum_N \exp\left[-j2\pi n\Delta x\left(\frac{\sin\theta}{\lambda} - \frac{\sin\theta_s}{\lambda_0}\right)\right]$$

where the total number of subarrays is M, and the subarray spacing is ΔS.

The subarray pattern and subarray AF are plotted in Figure 9-30 for the spectral components at band center and band edge. The subarray centers are more than a wavelength apart so the subarray AF will have grating lobes. At band center, the subarray pattern is not squinted, and the nulls of the subarray pattern will cancel the grating lobes of the subarray AF. At band edge, the subarray pattern will squint, will create a directivity loss in the main beam, and will no longer suppresses the subarray AF grating lobes. This is the compromise created by the time delayed subarray solution to the bandwidth problem. The trade-offs associated with subarray size, number of TDUs, scan loss, and grating lobes are part of the system design of any large wideband phased array radar [16].

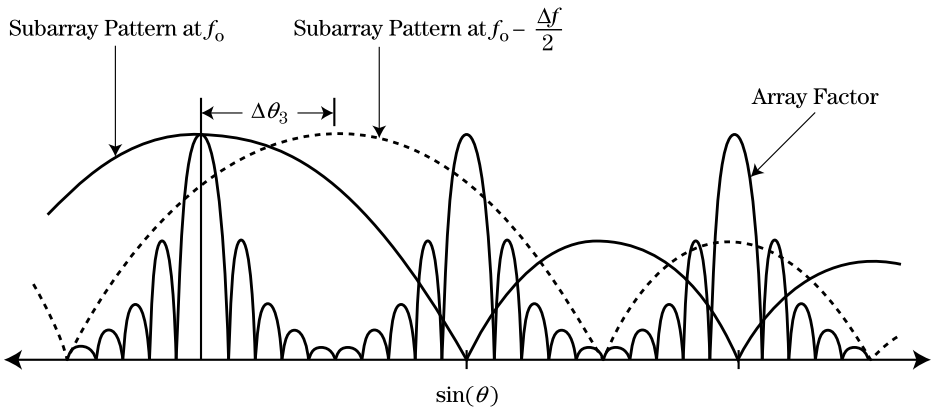

FIGURE 9-30 ■ For wideband operation the subarray pattern will squint, but the subarray AF will not.

9.8 ARRAY ARCHITECTURES

In modern radar systems the boundary between the antenna and other radar hardware is becoming less clear. With traditional systems there was a clear distinction between the receiver/exciter and the antenna. This is not so anymore. There has been a general trend to move the receiver/exciter electronics, and in some cases the signal processing, ever closer to the radiating surface of the antenna. This section will describe the most common array architectures as well as some emerging trends in antenna design.

9.8.1 Passive Array Architecture

The earliest phased array antenna systems used one large power amplifier (PA) tube to drive the entire array on transmit, and one low-noise amplifier (LNA) to set the noise figure after all array elements had been combined. This architecture is commonly referred to as a *passive phased array* because there is no amplification at the individual radiating element. The passive array architecture is shown in Figure 9-31.

The major benefit of the passive array is cost. There are, however, many pitfalls to this design that have led to a decline in its use. The passive architecture requires all array components to handle high power. Depending on the frequency and size of the array, there can be considerable loss in the combining network that will reduce the radar sensitivity. Lastly, TDUs are difficult to implement in this architecture because the array cannot conveniently be broken into subarrays; hence, passive arrays are not amenable to wideband applications.

9.8.2 Active Array Architecture

The dominant architecture at the time of this writing (2009) is the *active electrically scanned array* (AESA) where the final transmit power amplifier, receiver LNA, phase shifter, and possibly a programmable attenuator are packaged into a transmit/receive (T/R)

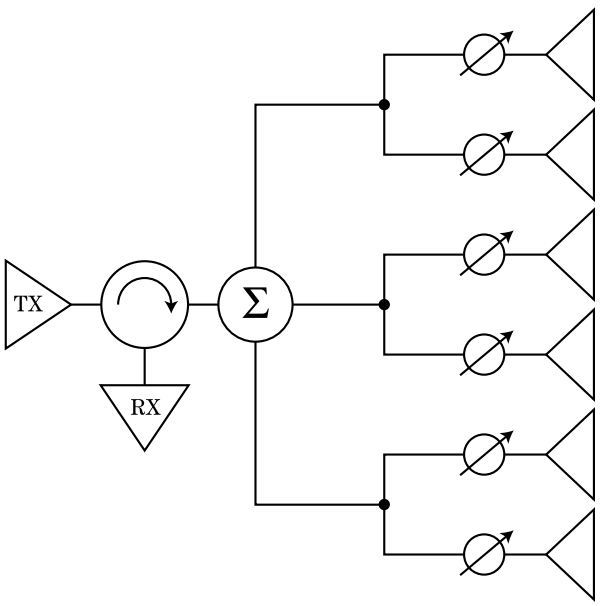

FIGURE 9-31 ■ The passive array uses one PA to drive the entire array and one LNA to set the noise figure.

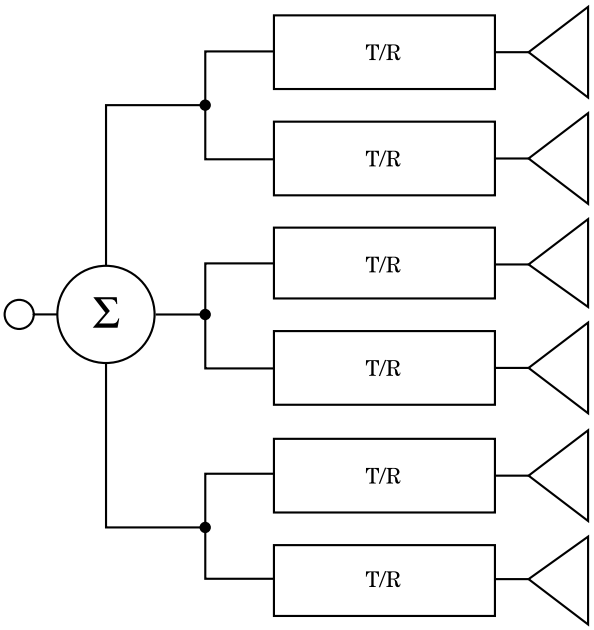

FIGURE 9-32 ■ An AESA places a PA and LNA behind each radiator. These electronics are usually packaged into a T/R module.

module behind each element [17,18]. This architecture, as shown in Figure 9-32, has several advantages over the passive architecture. Transmit losses between the PA and the radiator and receive losses between the radiator and the LNA are minimized. The AESA architecture provides additional beamforming flexibility since the amplitude and phase of each element can be dynamically controlled. This allows the aperture amplitude taper to be adjusted from pulse to pulse or from transmit to receive, whereas in a passive architecture the aperture amplitude taper is designed into the beamforming network of the array. The solid-state amplifiers can be broader band than tube amplifiers, and the received signal can be digitized or optically modulated to support digital or optical beamforming. AESAs can operate even when a small percentage of the T/R modules fail, so they degrade more gracefully than the passive architecture. Disadvantages of the AESA are cost, the requirement to cool the entire aperture to remove heat generated by the PAs, and the requirement for calibration in the field.

The cooling and cost problems may be alleviated for some applications by the emergence of the low power density (LPD) concept in which the TR module is reduced to the point where it becomes a single monolithic microwave integrated circuit (MMIC). Silicon-germanium is an ideal semiconductor technology for LPD applications because it is inexpensive, low power, and capable of excellent RF performance at typical radar frequencies [19–22].

Referring back to Figure 9-8, the required power-aperture product or power-aperture gain product of a LPD array is obtained by increasing the aperture size and reducing the transmit power. A diagonal line from the lower left corner to the upper right corner represents an aperture power density of 1 kW/m^2, which is generally considered the boundary between high and low power density. LPD AESAs have power densities low enough to eliminate the need for liquid cooling of the aperture. Although more T/R modules are required in LPD AESAs, the cost of the LPD T/R module will be significantly less than that of the high power T/R module. In LPD designs, large aperture is traded for high power, thus significantly reducing the prime power, cooling, and fuel requirements, which in turn can improve the radar's transportability.

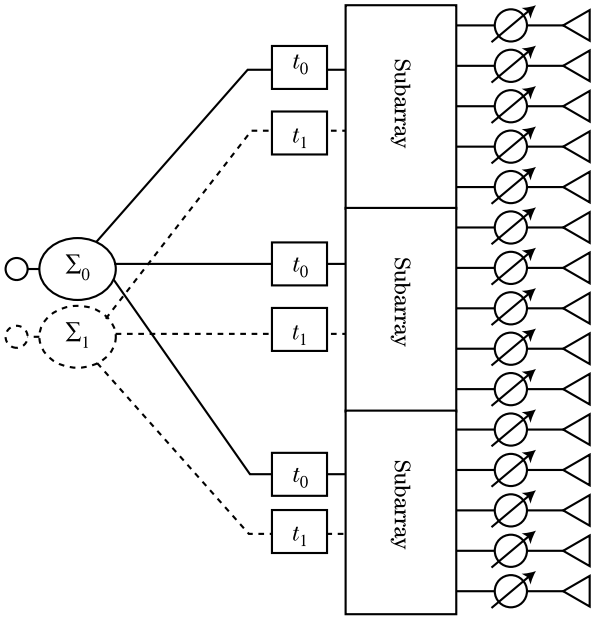

FIGURE 9-33 ■ An array divided into three subarrays. Different time delays are applied at the subarray level to form two simultaneous receive beams.

The LPD AESA is most beneficial in applications where aperture size is not fixed. For space-based or ground-based radars the antenna can be stowed for launch or transport and then erected for operation. LPD AESAs can also be used in aerostat or airship-based radars. LPD will obviously not work for radars that are severely spatially constrained, such as fighter aircraft radars.

9.8.3 Subarray Architecture

There are many variants of the subarray architecture, and one example is shown in Figure 9-33. In general, phase shift is applied at the radiating element, and amplification is applied to a grouping of elements referred to as a subarray. This makes the subarray architecture a hybrid of the passive and active architectures. Time delay is often implemented at the subarray level when the array is intended for wideband use. Time delay can be implemented with analog TDUs (as shown in Figure 9-33) or implemented digitally if the receive signal is digitized at the subarray. In addition, the subarray architecture has become a convenient method for implementing many advanced techniques such as digital beam forming and array signal processing. Many of these techniques are beyond the scope of this chapter; however, a brief introduction and relevant references will be provided [23–26].

The first advantage of the subarray is purely practical. Many modern phased arrays are manufactured using printed circuit board techniques for the radiating and beamforming layers. These techniques have size limitations that prohibit a large array from being manufactured in one piece. Subarrays are small, repeatable building blocks that can be mass produced and combined to form the full array. Figure 9-33 shows a 15-element array divided into three subarray units. The subarray units also offer a convenient location to implement time delay steering for wideband arrays as discussed in section 9.7.6.

The subarray architecture opens up additional opportunities when a digital receiver is placed behind each subarray or group of subarrays. Once the subarray outputs have been digitized, they can be weighted and combined in the digital computer to form, in principle,

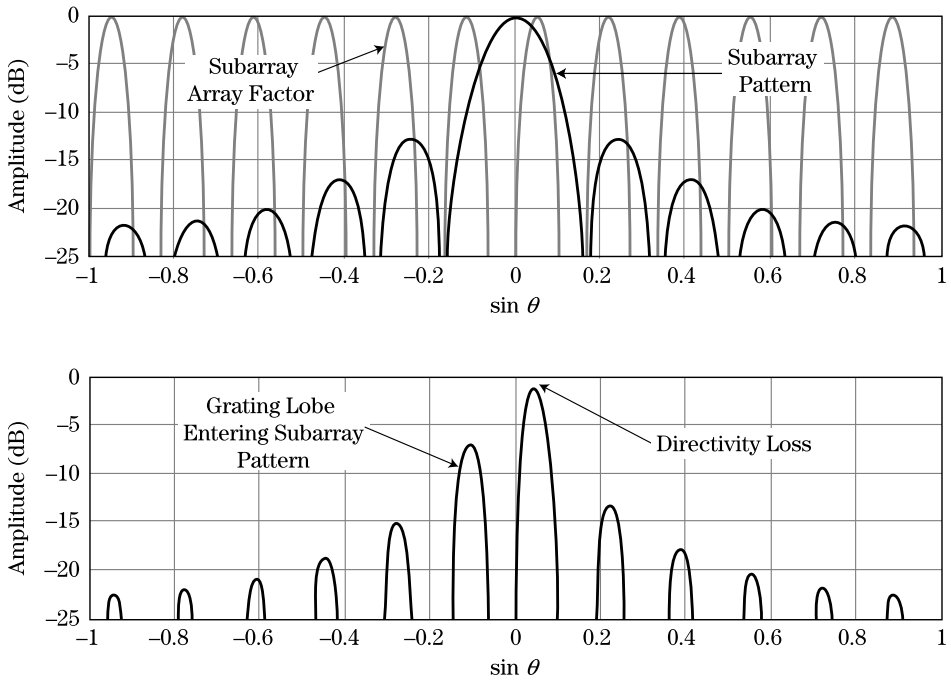

FIGURE 9-34 ■ During simultaneous beam operation the subarray pattern remains fixed, and the subarray AF will electronically scan. Grating lobes become significant when subarray AF lobes enter the subarray pattern mainlobe. Upper plot: Subarray pattern and subarray array factor. Lower: Combined antenna pattern.

an unlimited number of simultaneous offset beams without impacting radar resources or timeline.

Figure 9-33 shows the formation of two simultaneous beams using analog beamforming. For digital beamforming the analog TDUs would be replaced with digital receivers. Multiple simultaneous beams are commonly used to form clusters surrounding the main beam to improve the search timeline of a radar. The number of beams is limited only by the processing capabilities of the radar.

The extent that simultaneous receive beams can be offset from the primary, or center, receive beam is a function of the subarray beamwidth, and ultimately the subarray size. To explain this concept, remember that the radiation pattern of the array is the product of the element pattern, subarray pattern, and subarray AF. These contributors and the final radiation pattern are shown in Figure 9-34. The top figure shows the subarray AF and the subarray pattern. The bottom figure shows the combined antenna pattern.

During simultaneous beam operation, the element level phase shifters remain in the same state for all receive beams; thus, the subarray pattern does not scan. The receive beams can be digitally resteered, or offset, to anywhere within the subarray main beam by applying a phase shift or time delay at the subarray level. As discussed in section 9.7.3, grating lobes occur when array elements are spaced greater than $\lambda/2$ apart, which is certainly the case for the subarray centers. These subarray AF grating lobes are shown in the upper plot of Figure 9-34.

The majority of the grating lobes are not an issue because they are suppressed by the subarray pattern. However, during simultaneous beam operation, the grating lobes will scan and sometimes enter the subarray main beam that remains in a fixed position. Figure 9-34 shows a scenario where the subarray AF is scanned only three degrees yet the first grating lobe has entered the subarray main beam. Thus, the maximum offset angle for simultaneous beams is determined by the subarray AF grating lobes and the subarray pattern main beam.

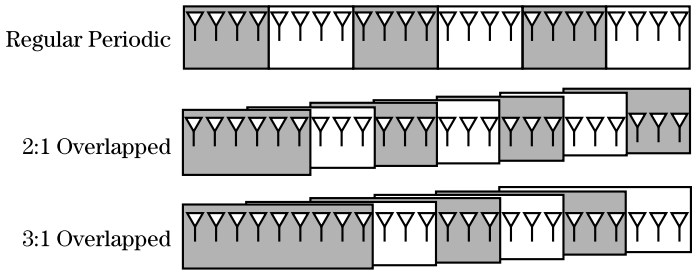

FIGURE 9-35 ■ Options for implementing the overlapped subarray architecture.

One method to increase the maximum offset angle is to create a narrower subarray beamwidth by using an overlapped subarray architecture. With overlapped subarrays each element will feed into more than one subarray receiver, hence increasing the subarray size without decreasing the number of subarrays. This concept is shown pictorially in Figure 9-35. The overlapped architecture creates larger subarray sizes, which result in narrower subarray patterns. Thus, simultaneous receive beams can be offset to larger angles without grating lobes entering the subarray pattern. This is just one of many benefits to the overlapped subarray architecture. A more through discussion of overlapped subarrays can be found in [27].

9.9 FURTHER READING

There are many superb textbooks devoted to the finer details of antenna design and analysis. Those by Johnson [1], Balanis [2], Stutzman [3] and Long [30] provide a thorough discussion of antenna fundamentals. However, these texts do not, nor were they intended to, address the design considerations of the modern radar antenna system. Most radar texts will designate a chapter specifically to the antenna system. A few excellent examples are chapter 9 of Skolnik [9] and chapters 37 and 38 of Stimson [28]. Finally, entire texts such as Mailloux [29] and Hansen [5] are devoted solely to the phased array antenna system.

The modern radar antenna is increasingly becoming a multidisciplinary system, and there are numerous emerging technologies of interest to the antenna engineer. References for these new technologies are placed throughout this chapter and can be found by monitoring the publications from the IEEE Antennas and Propagation Society and the IEEE Microwave Theory and Techniques Society.

9.10 REFERENCES

[1] Volakis, J., *Antenna Engineering Handbook*, 4d ed., McGraw-Hill Company, New York, 2007.

[2] Balanis, C.A., *Antenna Theory Analysis and Design*, 3d ed., John Wiley & Sons, Hoboken, NJ, 2005.

[3] Stutzman, W.L., and Thiele, G.A., *Antenna Theory and Design*, 2d ed., John Wiley & Sons, New York, 1998.

[4] Taylor, T.T, "Design of Line-Source Antennas for Narrow Beamwidth and Low Sidelobes," *IRE Transactions on Antennas and Propagation,* vol. AP-3, pp. 16–27, January 1955.

[5] Hansen, R.C., *Phased Array Antennas*, 2d ed., John Wiley & Sons, New York, 2010.

[6] Skolnik M.I., *Radar Handbook*, 3d ed., McGraw-Hill, New York, 2008.

[7] Sherman, S.M., *Monopulse Principles and Techniques*, Artech House, Dedham, MA, 1984.

[8] Bayliss, E.T., "Design of Monopulse Antenna Difference Patterns with Low Sidelobes," *Bell Systems Technical Journal,* vol. 47, pp. 623–650, 1968.

[9] Schell, A.C., "Antenna Developments of the 1950s to the 1980s," *IEEE Antennas and Propagation Society International Symposium,* vol. 1, pp. 30–33, July 8–13, 2001.

[10] Skolnik, M.I., *Introduction to Radar Systems,* 3d ed., McGraw Hill, New York, 2001.

[11] Maciel, J.J., Slocum, J.F., Smith, J.K., and Turtle, J., "MEMS Electronically Steerable Antennas for Fire Control Radars," *IEEE Aerospace and Electronic Systems Magazine,* vol. 22, pp. 17–20, November 2007.

[12] Brookner, E., "Phased Arrays around the World—Progress and Future Trends," *2003 IEEE International Symposium on Phased Array Systems and Technology,* pp. 1–8, Boston, MA, October 14–17, 2003.

[13] Brookner, E., "Phased-Array and Radar Breakthroughs," 2007 IEEE Radar Conference, pp. 37–42, April 17–20, 2007.

[14] Koul, S.K., and Bhat, B., *Microwave and Millimeter Wave Phase Shifters: Semiconductor and Delay Line Phase Shifters,* vol. 2, Artech House, Norwood, MA, 1992.

[15] Corey, L.E., "A Graphical Technique for Determining Optimal Array Geometry," *IEEE Transactions on Antennas and Propagation,* vol. AP-33, no. 7, pp. 719–726, July 1985.

[16] Howard, R.L., Corey, L.E., and Williams, S.P., "The Relationships between Dispersion Loss, Sidelobe Levels, and Bandwidth in Wideband Radars with Subarrayed Antennas," *1988 IEEE Antennas and Propagation Society International Symposium*, pp. 184–187, June 6–10, 1998.

[17] Cohen, E.D., "Trends in the Development of MMIC's and Packages for Active Electronically Scanned Arrays (AESAs)," *1996 IEEE International Symposium on Phased Array Systems and Technology,* pp. 1–4, October 15–18, 1996.

[18] Kopp, B.A., "S- and X-Band Radar Transmit/Receive Module Overview," *2007 IEEE Radar Conference,* pp. 948–953, April 17–20, 2007.

[19] Mitchell, M.A., Cressler, J.D., Kuo, W.-M.L., Comeau, J., and Andrews, J., "An X-Band SiGe Single-MMIC Transmit/Receive Module for Radar Applications," *IEEE 2007 Radar Conference,* pp. 664–669, April 17–20, 2007.

[20] Comeau, J.P., Morton, M.A., Wei-Min, L.K., Thrivikraman, T., Andrews, J.M. Grens, C., et al., "A Monolithic 5-Bit SiGe BiCMOS Receiver for X-Band Phased-Array Radar Systems," *IEEE Bipolar/BiCMOS Circuits and Technology Meeting, 2007,* pp. 172–175, September 30–October 2, 2007.

[21] Tayrani, R., Teshiba, M.A., Sakamoto, G.M., Chaudhry, Q., Alidio, R., Yoosin Kang, A., et al., "Broad-band SiGe MMICs for Phased-Array Radar Applications," *IEEE Journal of Solid-State Circuits,* vol. 38, no. 9, pp. 1462–1470, September 2003.

[22] Kane, B.C., Geis, L.A., Wyatt, M.A., Copeland, D.G., and Mogensen, J.A., "Smart Phased Array SoCs: A Novel Application for Advanced SiGe HBT BiCMOS Technology," *Proceedings of the IEEE,* vol. 93, no. 9, pp. 1656–1668, September 2005.

[23] Compton, R.T., *Adaptive Antennas: Concepts and Performance*, Prentice-Hall, Upper Saddle, River, NJ, 1988.

[24] Zatman, M., "Digitization Requirements for Digital Radar Arrays," *Proceedings of the 2001 IEEE Radar Conference,* pp. 163–168, May 1–3, 2001.

[25] Combaud, M., "Adaptive Processing at the Subarray Level," *Aerospace Science and Technology,* vol. 3, no. 2, pp. 93–105, 1999.

[26] Nickel, U., "Subarray Configurations for Digital Beamforming with Low Sidelobes and Adaptive Interference Suppression," *IEEE International Radar Conference,* pp. 714–719, 1995.

[27] Lin, C.-T., and Ly, H., "Sidelobe Reduction through Subarray Overlapping for Wideband Arrays," *Proceedings of the 2001 IEEE Radar Conference,* pp. 228–233, May 1–3, 2001.

[28] Stimson, G.W., *Introduction to Airborne Radar*, 2d ed., SciTech, Raleigh, NC, 1998.

[29] Mailloux, R.J., *Phased Array Antenna Handbook,* 2d ed., Artech House, Norwood, MA, 2005.

[30] Blake, L. and Long, M.W., *Antennas: Fundamentals, Design, Measurement*, 3d ed., SciTech, Raleigh, NC, 2009.

9.11 PROBLEMS

1. Assume an isotropic antenna has been invented that can transmit 10 watts. (a) Assume there is a 20 dBm^2 target 1 km away. What is the power density at this target? (b) Assume a large clutter object (RCS of 30 dBm^2) is located at the same range as the target but 20° away. Calculate the power density at the clutter location. (c) Why would this be a problem for the radar system?

2. Consider a radar antenna that has an aperture 3.0 m high by 3.5 m wide. Imagine a 10 GHz plane wave arriving from an angle of elevation = 0° and azimuth = 15°. (a) What is the total phase gradient across the aperture surface? (b) What if the azimuth angle is changed to 60°?

3. A fighter jet has a circular radar antenna in the nose of the aircraft that operates at 10 GHz. (a) Assuming the diameter is 1 meter and the aperture is uniformly illuminated, calculate the maximum directivity and beamwidth of the antenna. (b) How would these values change if the antenna operated at 32 GHz?

4. Consider a uniformly illuminated rectangular antenna with peak directivity of 35 dBi. What will the first sidelobe be in dBi? Now assume a −40 dB Taylor weighting is applied in the x-axis and a −25 dB Taylor weighting is applied in the y-axis. In dBi, what will the new peak directivity and peak sidelobe be? Assume the antenna aperture is error free.

5. A circular antenna with a diameter of 2 ft operates at 16 GHz. There are 2 dB of RF losses within the antenna and an RMS phase error of 15° on the aperture surface. Calculate the maximum directivity and gain of the antenna.

6. A radar system has been designed to track targets at range R. At the last minute the customer decides that she needs to track targets at $2R$, twice the initial range, and the remaining requirements must remain the same. The project manager decides to meet this new requirement by modifying the antenna. If aperture size is unchanged, by how much will transmit power be increased? What if the total transmit power remains constant and the aperture is increased? How much larger must the aperture be?

7. Assume a parabolic reflector is illuminated such that the edges of the reflector see 3 dB less power than the center of the reflector. Given a reflector diameter of 20 ft. and a focal length of 18 ft., how large must the feed aperture be if it is circular in shape and uniformly illuminated? The system operates at 10 GHz.

8. Consider a five-element linear array with element spacing of 0.5 wavelengths. Assume the path length from each element to summation point (φ_n) is equal. Using computational software (e.g., Matlab, Excel), plot the normalized array factor for incidence angles from −90° to +90°.

9. A linear array is to be designed that operates at 10 GHz and has a 1° beamwidth (assume uniform illumination). This array must electronically scan to 65° without grating lobes. What is will the element spacing be? How many elements will be used?

10. Consider a phased array that has a 3° beamwidth and 35 dBi of directivity at broadside. What are the beamwidth and directivity when the array is electronically scanned to 55°?

11. A 10 m space-based antenna is in low Earth orbit (LEO) at 1,000 km. The radar has an instantaneous bandwidth of 500 MHz and uses a phased array without time delay. Assuming that the antenna is calibrated in the center of the band, what is the pointing error at the edge of the instantaneous bandwidth when the antenna is electrically scanned to 50°? How many meters of pointing error does this translate too when mapped to the earth's surface? (Assume a flat earth to simplify this problem.)

12. For the scenario in question 11, assume time delay units are implemented instead of the phase shifters. How much time delay is required? What does this equal in phase?

13. Determine the mispointing error caused when a phase-shifter-based phased array electronically scans to 65°. Assume 10% instantaneous bandwidth and a center frequency of 3.5 GHz. What fraction of the beamwidth will this be if the antenna is 1 m long? What fraction of the beamwidth will this be if the antenna is 10 m long? Assume uniform aperture taper.

14. A phased array is to be designed that satisfies the following requirements at 10 GHz: (1) The antenna must have a broadside directivity of 35 dBi; (2) the array must have a square shape, uniform illumination, and a rectangular element grid; (3) the array must be able to scan to 30° in azimuth and 30° in elevation without grating lobes occurring; and (4) the array must meet the directivity requirement with 10° of random phase errors. How many elements are required to meet these requirements?

15. Assume that the requirements in question 14 have been changed such that low sidelobes are required for this aperture and it must electronically scan to more extreme angles. If a 40 dB Taylor weighting is applied to the aperture in both dimensions and the maximum scan angle is increased in both dimensions to 60°, how many elements must be used? Assuming $500 per element, how much additional cost is incurred?